ISSN 2310-6697
otoiser—open transactions on independent scientific-engineering research

FUNKTECHNIKPLUS # JOURNAL

Théorie—Expérimentation—Métrologie—Logiciel—Applications

ISSUE 39 — SATURDAY 31 JANUARY 2026 — YEAR 13

This small European Journal is
In the Defense of Honesty in Science and Ethics in Engineering

Period B'
Previous Period 2013-2024

Publisher
otoiser—open transactions on independent scientific engineering research
ARG IAOI NFI Lab—Antennas Research Group Informal Association Of Individuals No Finance Involved Laboratory
Scheiblingkirchen, Austria

Language — We emphasize the European Origins of our Journal by using English, German and French in its title, as well as, a Hellenic vignette in the front page. However, since we recognize the dominance of US English in the technical literature, we adopted it as the Journal's language.

Focus — We consider Radio—FUNK, which still creates a vivid impression of the untouchable, and its Technology—TECHNIK, from an Advanced—PLUS point of view, Plus—PLUS Telecommunications Engineering, Electrical Engineering and Computer Science, that is, we dynamically focus at any related scientific-engineering research regarding Théorie, Expérimentation, Métrologie, Logiciel, ou Applications.

Scope — We emphasize the scope broadness by extending the title of the Journal with a Doppelkreuz-Zeichen # which we use as a placeholder for the substitution of its disciplines

Frequency — Excluding *forces majeures,* we publish 3 issues per year: on 31st of January, on 31st of May, and on 30th of September.

Editions — We increase the edition number of an issue only when is absolutely needed to reform one or more of its papers——thus to increase their version numbers——but we keep unchanged its 1st edition date shown on its front page and we number its pages sequentially from 1. We count the editions of *About* separately.

Format — We use a fixed-space font, hyphenation, justification, unfixed word spacing, and the uncommon for Journals **A5** (half A4) page size to achieve WYSIWYG printing and clear reading of 2 to 4 side-by-side pages on wide-screen displays.

Editorial Group

About

Submissions

We can only consider papers written in the preferable and recommended odt format of LibreOffice, or even a paper in the MS Office with MathType doc format, if it would be proved that it is fully compatible with LibreOffice indeed.

Legal Notice — It is taken for granted that the submitter—correspondent author accepts, without any reservation, the totality of our publication conditions as they are analytically detailed here, in this *About*, as well as, that he also carries, in the case of a paper by multiple authors, the independent will of each one of his co-authors to unreservedly accept all the aforementioned conditions for their paper.

Electronic Publishing

We regularly use the Free Libre Open Source Software Libre Office with the Free Liberation Mono font and the Freewares PDFCreator and PDF-Xchange Viewer. We also use some basic html code of ours and the Free Open Digital Library of Internet Archive website, where we upload the FTP#J Collection of Issues, Paper reprints, *About* documents, and Volumes, in both portrait and landscape orientations, for download or very clear online reading with the Free Open Source BookReader.

Internet Addresses

Submissions : sub@ftpj.otoiser.org
Send Updates : updates@ftpj.otoiser.org

Paper Template : https://www.template.ftpj.otoiser.org
Reference Updates : https://www.updates.ftpj.otoiser.org
Internet Publishing : https://www.ftpj.otoiser.org

The FTP#J Collection at Internet Archive Digital Library :
https://archive.org/details/@funktechnikplusjournal

Please download the latest *About* edition from
https://about.ftpj.otoiser.org

Comments on RTV and HTV Materials for High Voltage Outdoor Insulation

M. G. Danikas and R. Sarathi

Independent Researcher, Formerly with
Democritus University of Thrace, School of Engineering,
Department of Electrical and Computer Engineering,
Power Systems Laboratory, 67100 Xanthi, Greece [1]

Indian Institute of Technology Madras, Department of
Electrical Engineering, High Voltage Laboratory,
Chennai, 600-036 India [2]

Abstract

The purpose of this short paper is to point out and comment on some aspects of silicone rubber materials used for outdoor insulators. The present note does not analyze in detail the properties of such insulating materials but it emphasizes factors affecting their performance.

Keywords

Silicone rubber, outdoor insulation, hydrophobicity, RTV silicone rubber, HTV silicone rubber, trihydrate alumina, arc resistance, low-molecular weight (LMW) polymer, corona discharges

Introduction

There is a vast body of technical literature regarding the RTV (Room Temperature Vulcanized) and HTV (High Temperature Vulcanized) polymer outdoor insulators [1] - [9]. In the last decades polymer insulators seem to replace traditional outdoor insulators made of porcelain and glass [10]. RTV and HTV silicone rubber seemed to be the preferred insulating material for outdoor high voltage applications [11]. Such materials are complex materials since they also include fillers in order to acquire a better arc resistance. Silicone rubber has a very important property, namely hydrophobicity.

Although the technology of polymer outdoor insulation proved to be reliable under various weather conditions, some questions w.r.t. to its particular characteristics need to be discussed. During the last decades, questions have been arisen. Pertinent questions as to the technology of both RTV and HTV rubber are:

1) Do fillers (such as Al_2O_3 $3H_2O$) influence negatively the mechanical properties of silicone rubber? Are the negative effects more pronounced for the RTV or for the HTV silicone rubber? Does a filler like Al_2O_3 $3H_2O$ benefit equally well HTV and RTV? If not, why is this so? Is there an optimum filler percentage which may give an optimum electrical performance for HTV? Is this optimum percentage different for RTV? If so, why?

2) Regarding hydrophobicity, is HTV more hydrophobic than RTV, or are they the same?

3) Is hydrophobicity due to low molecular weight degradation products or to unpolymerized monomer groups?

In this short paper, we will try to answer the above questions.

Comments and Discussion

Given that both the RTV and the HTV are complex materials, it can be said that fillers, such as Al_2O_3 $3H_2O$, generally improve the physical properties of the rubber in both its aforementioned types. There are, however, optimum levels of filler. Such an optimum level depends on factors such as base polymer, cure system, and possibly other formulation parameters. It must be emphasized that with proper formulating and processing, the fillers, such as trihydrate alumina (Al2O3 3H2O), can be incorporated into the rubber and can improve both the arc resistance and the physical properties. Having pointed the above, one cannot make a general statement, i.e. that Al_2O_3 $3H_2O$ benefits equally well HTV and RTV technologies. The benefit of the filler depends specifically on its type, amount and particle size as well as the quality of its dispersion and bonding within the matrix of the crosslinked polymer. Both formulating and processing issues are involved in achieving maximum benefit from the filler. There is an optimum level of filler for both HTV and RTV which is likely to be somewhat different. This again goes back to the specific chemical and processing technology employed. Utility people assume quite often that silicone rubber is a generic material and is all the same regardless of the specific and processing systems used. Although it is true that some generalizations can be made about the silicone family of rubber, from a formulation viewpoint it becomes much more difficult. Moreover, one must define what it is that is "optimized" by the filler. The optimization of arc resistance will likely lead to high levels of filler. However, this may lead to more filler than is actually needed since one of the unique characteristics of silicone is its ability to suppress the leakage currents which lead to the arcing. Therefore, optimizing the arc resistance alone may limit other properties of the material such as leakage current suppression or processing / handling properties.

Hydrophobicity is a property of paramount importance. This can vary not only between RTV and HTV but also within each group. Hydrophobicity is due to the methyl side groups on the silicone polymer backbone. It is also to be pointed out that factors such as curing system, filler loading and surface conditions affect the hydrophobicity. The aforementioned factors affect the loss and recovery rate of hydrophobicity under various stress conditions. Generally speaking, the hydrophobicity of the silicone family of materials is quite good. Whether or not meaningful performance distinctions (or predictions) can be made by use of the contact angle measurements depends. Explaining further this point, one can say that the performance of the material in a polluted environment depends not only on the hydrophobicity but also on the ability of the surface to encapsulate and transfer hydrophobicity to the surface pollutants [12].

As to the question whether hydrophobicity is due to low molecular weight (LMW) degradation products or to unpolymerized molecular groups, it can be said that hydrophobicity is probably due to LMW polymer which can migrate through the bulk rubber and can be driven to the surface in order to achieve thermodynamic equilibrium with the air on the surface. The surface energy of the LMW polymer is close to that of air and is therefore driven out to the surface. As this layer undergoes degradation through exposure to corona discharges, arcing and related phenomena, the methyl side groups on the polymer chains are oxidized to form a material with higher surface energy. The untreated

LMW material within the bulk of the rubber then is driven to the surface through microcracks in the top surface layer of reacted material by the thermodynamic driving force and thus restores the hydrophobicity. This LMW polymer is present in the rubber from its initial vulcanization. Whether or not additional LMW material is generated by degradation mechanisms is a subject to be further explored.

Although the above are mainly comments about silicone rubber insulators, such comments are also relevant to silicone rubber coatings. The question of hydrophobicity becomes even more acute for silicone rubber coatings since such coatings are very thin and, consequently, their reservoir of LMW polymer is not as rich as in typical silicone rubber insulators [13], [14]. Moreover, the question of the duration of hydrophobicity and its recovery is crucial also in the case of insulators consisting of silicone rubber - EPDM blends [15], [16], and also for superhydrophobic insulators [17], [18].

Conclusion

Although silicone rubber seems to be a reasonable alternative to traditional materials, such as porcelain and glass, questions as to the details of the processes during its manufacturing still remain. Although silicone rubber is a generic name, silicone rubber insulators’ performance depends on every single manufacturer’ processing. Hydrophobicity is a very important property for silicone rubber, however, its recovery or depletion depends on the severity of weather conditions. This holds especially true for silicone rubber coatings.

References – Updates – MD5 check

https://www.ftpj.otoiser.org/refs/391.htm

[1] Gorur R. S., "High voltage outdoor insulation technology", Control and Dynamic Systems, Vol. 44, Part 4, 1991, pp. 131 - 191

[2] Reynders J. P., Jandrell I. R., Reynders S. M., "Review of aging and recovery of silicone rubber insulation for outdoor use", IEEE Transactions on Dielectrics and Electrical Insulation, Vol. 6, No. 5, 1999, pp.620 - 631

[3] Hackam R., "Outdoor HV composite polymeric insulators", IEEE Transactions on Dielectrics and Electrical Insulation, Vol. 6, No. 5, 1999, pp. 557 - 585

[4] Danikas M. G., "Ageing properties of silicone rubber materials used in high voltage composite insulators", Journal of Electrical and Electronic Engineering, Australia, Vol. 15, No. 2, 1995, pp. 193 - 202

[5] Deng H., Hackam R., "Low-molecular weight silicone fluid in RTV silicone rubber coatings", IEEE Transactions on Dielectrics and Electrical Insulation, Vol. 6, No. 1, 1999, pp. 84 - 94

[6] Amin M., Akbar M., Amin S., "Hydrophobicity of silicone rubber used for outdoor insulation (an overview)", Reviews on Advanced Materials Science, Vol. 16, 2007, pp. 10 - 26

[7] Cherney E. A., "Silicone rubber dielectrics modified by inorganic fillers for outdoor high voltage insulation applications", IEEE Transactions on Dielectrics and Electrical Insulation, Vol. 12, No. 6, 2005, pp. 1108 - 1115

[8] Sarathi R., Chandrasekarr S., Yoshimura N., "Analysis of tracking phenomena in silicone rubber insulation material using moving average technique", Proceedings of the IEEE INDICON 2004 (First India Annual Conference 2004), 20-22 December 2004 https://doi.org/10.1109/INDICO.2004.1497712

[9] Chandrasekarr S., Sarathi R., Danikas M. G., "Analysis of surface degradation of silicone rubber insulation due to tracking under different voltage profiles", Electrical Engineering, Vol. 89, 2007, pp. 489 - 501

[10] Cojan M., Perret J., Malaguti C., Nicolini P., Looms J. S. T., Stannet A. W., "Polymeric transmission insulators: Their application in France, Italy and the UK", CIGRE Paper 22.10, 1980

[11] Danikas M. G., "Polymer outdoor insulators", Acta Electrotehnica Napocensis, Vol. 40, No. 1, 1999, pp. 3 - 10

[12] Toskey G. A., Private Communication, 10th January 1992

[13] Danikas M. G., Hackam R., "Discussion on: Low-molecular weight silicone fluid in RTV silicone rubber coatings", IEEE Transactions on Dielectrics and Electrical Insulation, Vol. 7, No. 3, 2000, pp. 461 - 462

[14] Sarathi R., Danikas M. G., "RTV silicone rubber coatings for outdoor insulators: A concise review of some factors affecting their behavior and some comments", Journal of Engineering Science and Technology Review, Vol. 14, No. 1, 2021, pp. 163 - 169

[15] Deepalaxmi R., Rajini V., "Performance evaluation of gamma irradiated SiR-EPDM blends", Nuclear Engineering and Design, Vol. 273, 2014, pp. 602 - 614

[16] Sykaras A, Rajini V., Danikas M. G., Sarathi R., "A study of SiR/EPDM mixtures for outdoor insulators", Engineering, Technology & Applied Science Research, Vol. 7, No. 4, 2017, pp. 1737 - 1740

[17] Wang Q., Liu S., Liu Sh., Zao Z, Gao Y., Wu C., Liang X., "Super-hydrophobic silicone rubber for outdoor electrical insulation", Nanotoday, Vol. 58, 2024 https://doi.org/10.1016/j.nantod.2024.102406

[18] Seyedmehdi S. A., Zhang H., Zhu J., "Superhydrophobic RTV silicone rubber insulator coatings", Applied Surface Science, Vol. 258, No. 7, 2012, pp. 2972 - 2976

A Conceptual Model for the Reflection Measurements of a Vector Network Analyzer System and its Practical Application

Nikolitsa I. Yannopoulou and Petros E. Zimourtopoulos

Antennas Research Group, Austria, EU - www.op4.eu

Abstract

We present the gradual building of our conceptual model for the reflection measurements of a VNA Vector Network Analyzer System. In this way, we reveal the fundamental idea behind this kind of measurements and prepare the studier for a deeper comprehension of this subject. Moreover, since this abstract model is exclusively based on technical specifications supplied by the manufacturers of system components, it is directly applicable in practice. To demonstrate this fact, we use a specific VNA System to compute and draw both the frequency dependent systematic error parameters of it and of the reflection coefficient and input impedance of a particular antenna we constructed and measured by using it.

Keywords

Microwave measurements, network analyzer, differential error region, differential error interval, S-parameters, calibration, antenna measurements, reflection measurements

Introduction

The measurement system of our conventional Vector Network Analyzer (VNA) with two measurement ports under Automated control via HPIB with the developed by us application [ANALYZE] and with an external signal generator to ensure the frequency stability through Phase-Locked Loop (PLL) characteristic is presented in Fig. 1. The well-known set-up of the reflection coefficient measurements of a Device Under Test (DUT) by using such a VNA is shown in detail in Fig. 2. The relation between the reflection coefficient of the DUT and its measured value can be mathematically described by the commonly accepted One Port Measurement Error Model

[1]. We thought that the necessarily abstract nature of this model obscures the relations between the involved quantities making difficult any further study. Although it seems that numerous articles have been appeared which describe a number of approaches to this measurement theory (e.g. [2] - [6]), these do not satisfy our demand for clearness. Therefore, we decided to attempt a different one overall examination of the measurement process in order to found our further research.

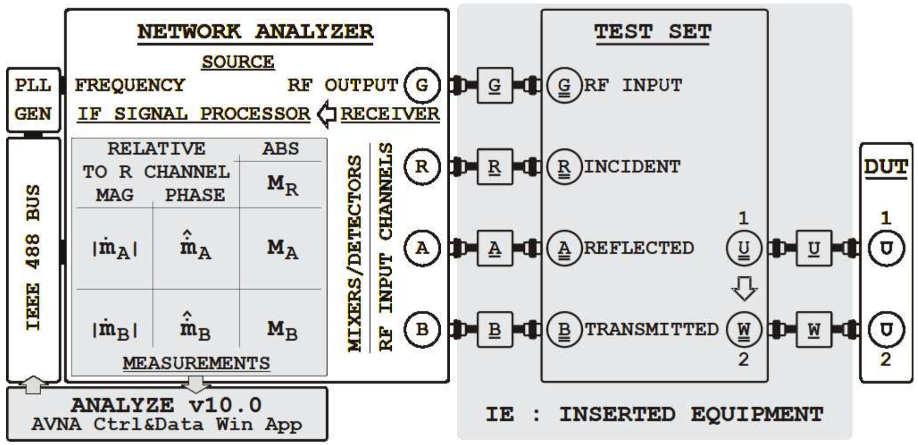

Fig. 1: Automated VNA measurement system

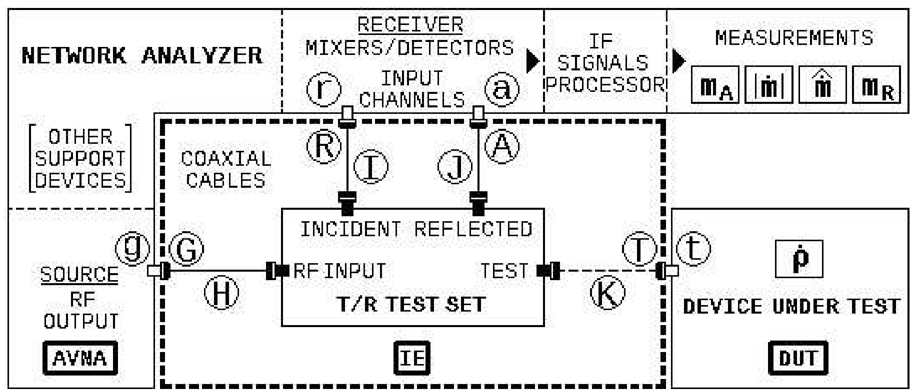

Fig. 2: Reflection measurements set-up

Analysis

We start our analysis considering that the measuring system consists of three distinct but interconnected parts accordingly to the amount of the available technical information.

The first part is active and contains the VNA itself plus any other supporting devices. The essential characteristic of this part is the great requirement for a complete analysis. Because of this complication, we have to base our study on overall external technical characteristics supplied by the manufacturer. In this way the VNA part can be described by a mathematical model of a rather theoretical nature.

The second part is the DUT itself. A model for this device consists of a single set definition for the considered reflection coefficient values.

The third part is passive and stands between the VNA and the DUT. We call this part "Inserted Equipment" (IE). A dashed bold line in Fig. 2 surrounds the IE part including the Transmission/Reflection Test Set (T/R) and the Coaxial Cables H, I, J and K. The K cable is added for the slightly more general case of a distanced DUT. The essential of the IE part is that it is capable of analysis based on technical characteristics supplied by the manufacturer.

In this way the IE part can be described by a mathematical model of a rather constructional nature. The model consists of an assembly of sets and functions. The three IE ports G, R, A are directly connected to the VNA ports g, r and a respectively and the fourth one T is connected to DUT port t. In these ports the models of the three parts have to interface each other by a set of mathematical relations.

Generally, the VNA source impresses a voltage to IE port G, which in the presence of the DUT reflection coefficient produces a pair of voltages to the VNA receiver ports, a and r.

After mixing and detecting the signals processor produces a quadruplet of measurements for the absolute amplitudes of the input signals and the amplitude and phase of their ratio. The existence of another input port B is connected to transmission measurements, therefore it is not involved here.

Theory

Let Z_0 be the system's characteristic impedance which is a constant positive real number, so we have

$$\boxed{Z_0 \in \mathbb{R}_+} \tag{1}$$

and from this

$$Y_0 \equiv \frac{1}{Z_0} \in \mathbb{R}_+ \tag{2}$$

Z_0 is the first of our model constants. We consider RMS values in the phasor notation for the involved quantities. In order to keep track of the used symbols we declare here the used notation: A dot over symbol represent complex quantity, a prime corresponds to the real part and a double prime to the imaginary part. Bold normal letters are used to define sets while bold italic define functions.

At each port x of the measurement system of Fig. 2, where

$$x = g,\ a,\ r,\ t,\ G,\ A,\ R,\ T \tag{3}$$

we consider the levels of the "normalized" [7] incoming $\dot a_x$ and outgoing $\dot b_x$ wave values at this x port, as they are defined by the relations

$$\dot a_x = \frac{\dot V_x + Z_0 \dot I_x}{2\sqrt{Z_0}},\ \ \dot b_x = \frac{\dot V_x - Z_0 \dot I_x}{2\sqrt{Z_0}} \tag{4}$$

where

$$\dot a_x = a_x' + i\, a_x'',\ \ \dot b_x = b_x' + i\, b_x''$$

so that the following relations are valid:

$$\dot V_x = \sqrt{Z_0}(\dot a_x + \dot b_x), \tag{5a}$$

$$\dot I_x = \sqrt{Y_0}(\dot a_x - \dot b_x) \tag{5b}$$

$$\dot V_{a_x} \equiv \sqrt{Z_0}\,\dot a_x,\ \ \dot V_{b_x} \equiv \sqrt{Z_0}\,\dot b_x, \tag{6a}$$

$$\dot I_{a_x} \equiv \sqrt{Y_0}\,\dot a_x,\ \ \dot I_{b_x} \equiv -\sqrt{Y_0}\,\dot b_x \tag{6b}$$

$$\dot V_x = \dot V_{a_x} + \dot V_{b_x},\ \ \dot I_x = \dot I_{a_x} + \dot I_{b_x} \tag{7}$$

$$\dot P_{a_x} \equiv \dot V_{a_x} \overset{*}{\dot I}_{a_x} = a_x^2 = P'_{a_x} \ge 0, \tag{8a}$$

$$P''_{a_x} = 0 \tag{8b}$$

$$\dot P_{b_x} \equiv \dot V_{b_x} \overset{*}{\dot I}_{b_x} = -b_x^2 = P'_{b_x} \le 0, \tag{9a}$$

$$P''_{b_x} = 0 \tag{9b}$$

$$\dot P_x = (\dot V_x \overset{*}{\dot I}_x) = (\dot a_x + \dot b_x)(\dot a_x - \dot b_x)^* = \\ = (|\dot a_x|^2 - |\dot b_x|^2) - 2i(\dot a_x \overset{*}{\dot b}_x)'' \tag{10}$$

$$P'_x \equiv (\dot P_x)' = (\dot V_x \overset{*}{\dot I}_x)' = |\dot a_x|^2 - |\dot b_x|^2 = \\ = a_x^2 - b_x^2 = P'_{a_x} + P'_{b_x} \tag{11}$$

$$\dot\rho_x \equiv \dot\rho_{V_x} \equiv \frac{\dot V_{b_x}}{\dot V_{a_x}} = \frac{\dot b_x}{\dot a_x} \tag{12a}$$

$$\dot\rho_{I_x} \equiv \frac{\dot I_{b_x}}{\dot I_{a_x}} = -\frac{\dot b_x}{\dot a_x} = -\dot\rho_x \tag{12b}$$

$$\dot V_{a_x} \ne 0,\ \ \dot a_x \ne 0 \tag{12c}$$

and especially for an one port only passive network

$$0 \le P^{'} = a^2 - b^2 = a^2\left(1 - \frac{b^2}{a^2}\right) \Rightarrow$$

$$\Rightarrow 0 \le 1 - \frac{b^2}{a^2} = 1 - \rho^2 = (1+\rho)(1-\rho)$$

$$\Rightarrow 0 \le \rho^2 \le 1 \Rightarrow 0 \le \rho \le 1 \qquad (13)$$

so that for all one port passive networks or loads we have

$$\boxed{\boldsymbol{\dot\rho} \equiv \{\dot\rho \mid 0 \le |\dot\rho| \le 1 \subset \dot{\mathbb{C}}} \qquad (14)$$

We consider this set as one of the involved sets in our model, while

$$\frac{\dot P_b}{\dot P_a} = \frac{P^{'}_b}{P^{'}_a} = \frac{\dot V_b \overset{*}{\dot I_b}}{\dot V_a \overset{*}{\dot I_a}} = \left(\frac{\dot V_b}{\dot V_a}\right)\left(\frac{\overset{*}{\dot I_b}}{\overset{*}{\dot I_a}}\right) =$$

$$= \dot\rho_V \overset{*}{\dot\rho_I} = \dot\rho_V\left(-\overset{*}{\dot\rho_V}\right) =$$

$$= -|\dot\rho_V|^2 = -\frac{b^2}{a^2} = -\rho^2 \qquad (15)$$

and in each interconnection of the ports x (g, a, r, t), and X (G, A, R, T), we have the interface relations:

$$\dot V_X = \dot V_x,\ \ \dot I_X = -\dot I_x,$$

$$\dot a_X = \dot b_x,\ \ \dot b_X = \dot a_x, \qquad (16)$$

$$\dot P_X = -\dot P_x,\ \ P^{'}_X = -P^{'}_x\ \ P^{''}_X = -P^{''}_x$$

A. The VNA

The first part can be described from the available VNA technical specifications, which can be qualified by properly defined sets.

A1. Frequency range

If f_m and f_M are the minimum and maximum operating frequencies respectively then

$$\boxed{\begin{aligned}\mathbf{f} &\equiv [f_m, f_M] = \\ &= \{f \mid 0 < f_m \le f \le f_M\} \subset \mathbb{R}_+\end{aligned}} \qquad (17)$$

We consider the f as the first independent variable of our model, with values in the above real interval.

A2. The Source

We interpret the technical characteristics for the output power by the equivalence shown in Fig. 3 under the ideal conditions. We will use the VNA source to feed passive loads exclusively.

After the above relations we have obviously from Fig. 3 at ports g, G:

$$\dot b_g = \dot a_G = \dot\rho_S \dot a_g + \frac{(1-\dot\rho_S)}{2}\dot e_S =$$

$$= \dot\rho_S \dot b_G + \frac{(1-\dot\rho_S)}{2}\dot e_S,\ \ \dot e_S \equiv \frac{\dot E_S}{\sqrt{Z_0}} \qquad (18)$$

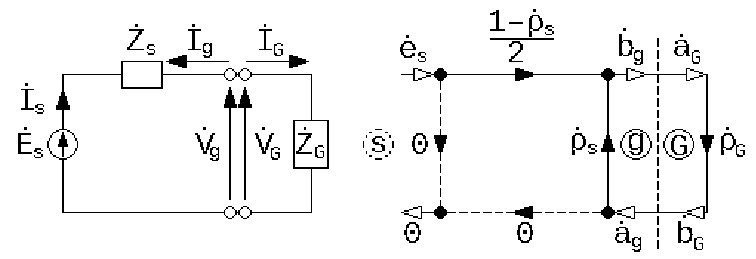

Fig. 3: One port S-parameter flow graph equivalent for a voltage source

for every source reflection coefficient $\dot\rho_S \in \boldsymbol{\dot\rho}_S$ and

$$\boldsymbol{\dot\rho}_S \equiv \{\dot\rho \mid (\dot\rho \in \boldsymbol{\dot\rho})\ \&\ (\rho \ne 1)\} \subset \boldsymbol{\dot\rho} \qquad (19)$$

which obviously in general can contain every reflection coefficient value except of an open circuit. By rearranging (18) taking into account that

$\dot b_G = \dot\rho_G \dot a_G$ we have

$$2(1 - \dot\rho_S\dot\rho_G)\dot a_g = (1 - \dot\rho_S)\dot e_S \qquad (20)$$

$$\dot\rho_G \in \boldsymbol{\dot\rho}_G \equiv \{\dot\rho \mid (\dot\rho \in \boldsymbol{\dot\rho})\&(\rho < 1)\} \subset \boldsymbol{\dot\rho} \qquad (21)$$

The last one can be used to define the function:

$$\boldsymbol{e}_S : \boldsymbol{\dot\rho}_S \times \boldsymbol{\dot\rho}_G \times \mathbb{R}_+ \to \mathbb{R}_+; \qquad (22)$$

$$\forall \dot\rho_S \in \boldsymbol{\dot\rho}_S,\ \forall \dot\rho_G \in \boldsymbol{\dot\rho}_G,\ \forall P \exists!\, P^{'}_G \in \mathbb{R}_+$$

$$e_S(\dot\rho_S, \dot\rho_G, P^{'}_G) = \frac{2\,|1-\dot\rho_S\dot\rho_G|}{\sqrt{(1-\rho_G^2)}\,|1-\dot\rho_S|}\sqrt{P^{'}_G}$$

As we described the VNA's source as a voltage source in the way shown in Fig. 3 and equivalently by the one-port S-parameter flow graph, it is possible to include a quantitative description of the RF source level in dBm by the well known relation

$$\tilde P[\mathrm{dBm}] \equiv 10\log\frac{P[\mathrm{W}]}{10^{-3}[\mathrm{W}]} \qquad (23)$$

via the constantly real average power P_S to port S which includes a constant amplitude incoming without any outgoing wave. We consider the $\tilde P_0[\mathrm{dBm}]$ as the second independent variable of the model from which the value of the voltage source can be defined by the interval:

$$\boxed{\tilde{\mathbf{P}}_0 \equiv [\tilde P_{0_m}, \tilde P_{0_M}] \subset \mathbb{R}_+} \qquad (24)$$

where $\tilde P_{0_m}, \tilde P_{0_M}$ are the minimum and maximum output power levels in dBm as they are defined in manufacturer's characteristics, where as usual we have in general:

$$P_0 = 10^{-3}10^{\frac{\tilde{P}_0}{10}} \quad (25)$$

Then we can define the functions

$$\boldsymbol{e}_0 : \tilde{\mathbf{P}}_0 \to \mathbb{R}_+ ; \forall \tilde{P}_0 \in \tilde{\mathbf{P}}_0, \exists ! e_0 \in \mathbb{R}_+,$$

$$e_0 \equiv \boldsymbol{e}_0(\tilde{P}_o) \equiv \boldsymbol{e}_S(\dot{\rho}_S = 0, \dot{\rho}_G = 0, P'_G = P_0 = 10^{-3}10^{\frac{\tilde{P}_0}{10}}) =$$

$$= 2\sqrt{10^{-3}}10^{\frac{\tilde{P}_0}{20}} \quad (26)$$

$$\boldsymbol{E}_0 : \tilde{\mathbf{P}}_0 \to \mathbb{R}_+ ; \forall \tilde{P}_0 \in \tilde{\mathbf{P}}_0, \exists ! E_0 \in \mathbb{R}_+,$$

$$E_0 \equiv \boldsymbol{E}_0(\tilde{P}_0) \equiv \sqrt{Z_0}\boldsymbol{e}_0(\tilde{P}_0) =$$

$$= 2\sqrt{10^{-3}Z_0}10^{\frac{\tilde{P}_0}{20}} \quad (27)$$

$$\mathbf{E}_0 \equiv \boldsymbol{E}_0[\tilde{\mathbf{P}}_0] \quad (28)$$

$$\hat{\mathbf{E}}_0 \equiv (-\pi, \pi] \quad (29)$$

$$\dot{\boldsymbol{E}}_0 : \tilde{\mathbf{P}}_0 \times (-\pi, \pi] \to \mathbb{C} \quad (30)$$

$$\dot{\mathbf{E}}_0 \equiv \{\dot{E}_0 \equiv E_0 e^{i\hat{E}_0} \mid (E_0 \in \mathbf{E}_0) \& (\hat{E}_0 \in \hat{\mathbf{E}}_0)\} \quad (31)$$

$$\dot{\boldsymbol{e}}_0 : \tilde{\mathbf{P}}_0 \times (-\pi, \pi] \to \mathbb{C};$$

$$\dot{\boldsymbol{e}}_0 \equiv \frac{1}{Z_0}\dot{\boldsymbol{E}}_0 \quad (32)$$

and another one function for the impressed voltage source so that

$$\mathbf{e}_g \equiv [e_{g_m}, e_{g_M}] = \{e_g \equiv |\dot{e}_g| : 0 < e_{g_m} \le e_g \le e_{g_M}\} \subset \mathbb{R}_+ \quad (33)$$

We consider an undetermined but constant value for the phase $\hat{E}_g$ of the voltage source and finally

$$\dot{\mathbf{e}}_g \equiv \{\dot{e}_g \equiv e_g e^{i\hat{e}_g} \mid (e_g \in \mathbf{e}_g) \& \hat{e}_g \in (-\pi, \pi]\} \quad (34)$$

For passive load connected to port G, with a reflection coefficient $\dot{\rho}_G$, we have, as before, a voltage drop

$$\dot{\mathbf{e}}_G \equiv \{\dot{e}_G \equiv e_G e^{i\hat{e}_G} \mid (e_G \in \mathbf{e}_G) \& \hat{e}_G \in (-\pi, \pi]\} \quad (35)$$

A3. The Receiver Inputs

We accept that do not take into account any dependence of the output voltage from the frequency because it is always possible to adjust the receiver inputs independently in a way that always guarantees that the output voltage lies between the above values. The frequency f and the output voltage levels E are the VNA’s independent variables. If we admit, for simplicity, that the input channels are independent but they have identical characteristics for the maximum permissible input level V_{i_M} and the minimum detectable level above some noise floor V_{i_m} then, as above, we have:

$$\mathbf{V}_i \equiv [V_{i_m}, V_{i_M}] = \{V_i \equiv |\dot{V}_i| : 0 < V_{i_m} \le V_i \le V_{i_M}\} \subset \mathbb{R}_+ \quad (36)$$

$$\hat{\mathbf{V}}_i \equiv (-\pi, \pi] = \{\hat{V}_i \equiv \sphericalangle \dot{V}_i \mid -\pi < \hat{V}_i \le \pi\} \subset \mathbb{R} \quad (37)$$

$$\dot{\mathbf{V}}_i \equiv \{\dot{V}_i \equiv V_i e^{i\hat{V}_i} \mid (V_i \in \mathbf{V}_i) \& (\hat{V}_i \in \hat{\mathbf{V}}_i)\} \subset \mathbb{C} \quad (38)$$

so at the input ports a and r

$$\mathbf{V}_a = \mathbf{V}_r = \mathbf{V}_i \quad (39)$$

$$\hat{\mathbf{V}}_a = \hat{\mathbf{V}}_r = \hat{\mathbf{V}}_i \quad (40)$$

$$\dot{\mathbf{V}}_a = \dot{\mathbf{V}}_r = \dot{\mathbf{V}}_i \quad (41)$$

$$\tilde{\mathbf{P}}_i \equiv [\tilde{P}_{i_m}, \tilde{P}_{i_M}] \subset \mathbb{R}_+ \quad (42)$$

A4. The measurement ranges

A4a. Magnitude

The measurements concern the magnitude of the input signals at A, R ports and the magnitude and phase of their ratio. In the same manner as above, we have for the magnitude

$$\tilde{\mathbf{M}}_i \equiv [\tilde{M}_{i_m}, \tilde{M}_{i_M}] = \{\tilde{M}_i \mid 0 < \tilde{M}_{i_m} \le \tilde{M}_i \le \tilde{M}_{i_M}\} \subset \mathbb{R}_+ \quad (43)$$

$$\tilde{\mathbf{M}}_a = \tilde{\mathbf{M}}_r = \tilde{\mathbf{M}}_i \quad (44)$$

and for the ratio

$$\tilde{\mathbf{m}}_i \equiv [\tilde{m}_m, \tilde{m}_M] = \{\tilde{m} \mid 0 < \tilde{m}_m \le \tilde{m} \le \tilde{m}_M\} \subset \mathbb{R}_+ \quad (45)$$

$$\hat{\mathbf{m}} \equiv (-\pi, \pi] = \{\hat{m} \equiv \sphericalangle \dot{m} \mid -\pi < \hat{m} \le \pi\} \subset \mathbb{R} \quad (46)$$

hence

$$\dot{\mathbf{m}} \equiv \{\dot{m} \equiv 10^{\frac{\tilde{m}}{20}} e^{i\hat{m}} \mid (\tilde{m} \in \tilde{\mathbf{m}}) \& (\hat{m} \in \hat{\mathbf{m}})\} \subset \mathbb{C} \quad (47)$$

A5. Measurement operation

A5a. Input channel Magnitude measurement

If we consider for each input channel A, R the functions

$$\boldsymbol{M}_A : \mathbf{f} \times \mathbf{V}_A \to \mathbf{M}_A \quad (48)$$

$$\boldsymbol{M}_R : \mathbf{f} \times \mathbf{V}_R \to \mathbf{M}_R \quad (49)$$

but

$$\dot{\mathbf{V}}_A = \dot{\mathbf{V}}_R = \dot{\mathbf{V}}_i \quad (50)$$

$$\mathbf{M}_A = \mathbf{M}_R = \mathbf{M}_i \quad (51)$$

and if

$$\boldsymbol{M}_i : \mathbf{f} \times \mathbf{V}_i \to \mathbf{M}_i \quad (52)$$

such that

$$\boldsymbol{M}_A = \boldsymbol{M}_R = \boldsymbol{M}_i \tag{53}$$

obviously

$$V_i^2 = Z_0(a_i^2 + b_i^2 + 2(\dot{a}_i \overset{*}{\dot{b}_i})') = $$

$$= Z_0(1 + \rho_i^2 + 2\dot{\rho}_i')a_i^2 \tag{54}$$

The ρ_i has a value rather far away from unit, so that

$$0 < 1 - \rho_i^2 \tag{55}$$

$$-\dot{\rho}_i' \le |\dot{\rho}_i'| \le \rho_i < 1 \Rightarrow 1 + \rho_i^2 + 2\dot{\rho}_i' =$$

$$= (1 + \dot{\rho}_i')^2 + \dot{\rho}_i''^2 > 0 \tag{56}$$

$$\dot{P}_i' \equiv (\dot{V}_i \overset{*}{\dot{I}_i})' = a_i^2 - b_i^2 = (1 - \rho_i^2)\, a_i^2 =$$

$$= \frac{(1 - \rho_i^2)}{(1 + \rho_i^2 + 2\dot{\rho}_i')}(\frac{1}{Z_0})V_i^2 \tag{57}$$

replacing a_i^2 from (54). Then be setting τ_i with (58) we get expression (59) for V_i:

$$\tau_i \equiv \sqrt{10^{-3}\, Z_0 \frac{(1 + \rho_i^2 + 2\dot{\rho}_i')}{(1 - \rho_i^2)}} \tag{58}$$

$$V_i = \tau_i\, 10^{\frac{\dot{P}_i'^{[dBm]}}{20}} \tag{59}$$

We suppose that we have available the (relative) magnitude frequency response for the magnitude of the input signal which in fact suggests linearity of the M function into the $\dot{V}_i$ variable:

$$K_i^{[dB]}(f) \equiv M_i^{[dBm]}(f, 0^{[dBm]}) - M_i^{[dBm]}(f_0, 0^{[dBm]}) \tag{60}$$

$$A_i^{[dB]}(f) \equiv K_i^{[dB]}(f) + M_i^{[dBm]}(f_0, 0^{[dBm]}) \tag{61}$$

$$M_i^{[dBm]}(f, \dot{P}_i'^{[dBm]}) = A_i^{[dB]}(f) + \dot{P}_i'^{[dBm]} \tag{62}$$

$$V_i = (\tau_i\, 10^{\frac{-A^{[dB]}(f)}{20}})\, 10^{\frac{M_i^{[dBm]}(f, \dot{P}_i'^{[dBm]})}{20}} \tag{63}$$

Thus, we define a function

$$\boldsymbol{K}_i : \mathbf{f} \to \mathbf{A}_i;\ K_i = K_i(f) \equiv \tag{64}$$

$$\equiv \frac{M_i(f_i, V_{i_0})}{M_i(f_0, V_{i_0})} = (\frac{1}{M_{i_0}})M_i(f_i, V_{i_0})$$

where

$$M_{i_0} = M_i(f_0, V_{i_0}) \tag{65}$$

This suggests that linearity can be assumed to be hold in the second variable V_i:

$\forall f \in \mathbf{f},\ \forall V_i \in \mathbf{V}_i,\ \exists!\, M_i \in \mathbf{M}_i,$

$$M_i = M_i(f, V_i) = M_i(f, V_i(\frac{V_{i_0}}{V_{i_0}})) =$$

$$= M_i(f, (\frac{V_i}{V_{i_0}})V_{i_0}) =$$

$$= (\frac{V_i}{V_{i_0}})\, M_i(f, V_{i_0}) =$$

$$= (\frac{V_i}{V_{i_0}})\, M_i(f, V_i = V_{i_0}) = \tag{66}$$

$$= (\frac{V_i}{V_{i_0}})\, M_{i_0} K_i(f) = (\frac{M_{i_0}}{V_{i_0}})K_i(f)V_i$$

In this way, we can define the function

$$\boldsymbol{A}_i : \mathbf{f} \to \mathbb{R} \tag{67}$$

$\forall f \in \mathbf{f},\ \exists!\, k \in \mathbb{R},$

$$k = A_i(f) \equiv (\frac{M_{i_0}}{V_{i_0}})K_i(f) \tag{68}$$

so that finally

$\forall f \in \mathbf{f},\ \forall V_i \in \mathbf{V}_i,\ \exists!\, M_i \in \mathbf{M}_i,$

$$M_i = M_i(f, V_i) = A_i(f)V_i \tag{69}$$

A5b. Input signals ratio measurements

Initially we define the ratio of the input signals from the

$$\dot{\boldsymbol{v}} : \dot{\mathbf{V}}_A \times \dot{\mathbf{V}}_R \to \mathbb{C} \tag{70}$$

$\forall \dot{V}_A \in \dot{\mathbf{V}}_A,\ \forall \dot{V}_R \in \dot{\mathbf{V}}_R,$

$$\dot{v} = \dot{v}(\dot{V}_A, \dot{V}_R) \equiv \frac{\dot{V}_A}{\dot{V}_R} \text{ with } \dot{V}_R \ne \dot{0} \tag{71}$$

so that the set of resulting values is the image

$$\dot{\mathbf{v}} \equiv \dot{\boldsymbol{v}}\,[\, \dot{\mathbf{V}}_A \times \dot{\mathbf{V}}_R\,] \tag{72}$$

After this we have for the magnitude of the ratio:

$$\mathbf{v} \equiv [\, v_m, v_M\,] = \{ v \equiv |\dot{v}|\ |\ (0 < v_m \equiv$$

$$\equiv \frac{V_{i_m}}{V_{i_M}} \le v \le v_M \equiv \frac{V_{i_M}}{V_{i_m}})\} \subset \mathbb{R}_+ \tag{73}$$

Let

$$\hat{V} \equiv \hat{V}_A - \hat{V}_R \tag{74}$$

then the phase of $\dot{v}$ is

$$\hat{v} \equiv \measuredangle(\frac{\dot{V}_A}{\dot{V}_R}) \tag{75}$$

which belongs to the set $\hat{\mathbf{v}}$ defined by the following property:

$$\hat{V} \in \left\{ \begin{array}{l} (-2\pi, -\pi\,] \\ (\pi, +\pi\,] \\ (\pi, 2\pi\,] \end{array} \right\} \Rightarrow \hat{v} = \hat{V} + \left\{ \begin{array}{r} 2\pi \\ 0 \\ -2\pi \end{array} \right. \tag{76}$$

The ratio measurements can be described now by the functions:

$$\boldsymbol{m} : \mathbf{f} \times \mathbf{v} \to \mathbf{m} \tag{77}$$

and

$$\hat{\boldsymbol{m}} : \mathbf{f} \times \hat{\mathbf{v}} \to \hat{\mathbb{m}} \qquad (78)$$

so the measurements can be represented by the function

$$\dot{\boldsymbol{m}} : \mathbf{f} \times \dot{\mathbf{v}} \to \dot{\mathbb{m}};\ \forall\, \mathrm{f} \in \mathbf{f},\ \forall\, \dot{\mathrm{v}} \in \dot{\mathbf{v}},$$

$$\dot{m}(\mathrm{f}, \dot{\mathrm{v}}) \equiv m(\mathrm{f}, \mathrm{v}) e^{i \hat{m}(\mathrm{f}, \hat{\mathrm{v}})} \qquad (79)$$

It is supposed now, that we have available a magnitude and a phase relative frequency responses from the two different input channels (fa, fb), which, as above, can be described by the functions:

$$\boldsymbol{k} : \mathbf{f} \to \mathbb{R};\ \forall\, \mathrm{f} \in \mathbf{f},\ \exists!\, \mathrm{k} \in \mathbb{R},$$

$$\mathrm{k} = k(\mathrm{f}) \equiv \frac{m(\mathrm{f}, \mathrm{v}_0)}{m(\mathrm{f}_a, \mathrm{v}_0)} \qquad (80)$$

$$\hat{\boldsymbol{k}} : \mathbf{f} \to \mathbb{R};\ \forall\, \mathrm{f} \in \mathbf{f},\ \exists!\, \hat{\mathrm{k}} \in \mathbb{R}, \qquad (81)$$

$$\hat{\mathrm{k}} = \hat{k}(\mathrm{f}) \equiv \hat{m}(\mathrm{f}, \hat{\mathrm{v}}_0) - \hat{m}(\mathrm{f}_b, \hat{\mathrm{v}}_0) + \nu(2\pi)$$

where

$$\nu \in \{-1, 0, 1\} \qquad (82)$$

as above, in order to keep $\hat{\mathrm{k}}$ into $(-\pi, \pi]$.

$$\dot{\boldsymbol{k}} : \mathbf{f} \to \dot{\mathbb{C}};\ \forall\, \mathrm{f} \in \mathbf{f},\ \exists!\, \dot{\mathrm{k}} \in \dot{\mathbb{C}},$$

$$\dot{\mathrm{k}} = \dot{k}(\mathrm{f}) \equiv k(\mathrm{f}) e^{i \hat{k}(\mathrm{f})} =$$

$$= \frac{m(\mathrm{f}, \mathrm{v}_0)}{m(\mathrm{f}_a, \mathrm{v}_0)} e^{i(\hat{m}(\mathrm{f}, \hat{\mathrm{v}}_0) - \hat{m}(\mathrm{f}_b, \hat{\mathrm{v}}_0))} e^{i\nu(2\pi)} =$$

$$= \frac{m(\mathrm{f}, \mathrm{v}_0) e^{i \hat{m}(\mathrm{f}, \hat{\mathrm{v}}_0)}}{m(\mathrm{f}_a, \mathrm{v}_0) e^{i \hat{m}(\mathrm{f}_b, \hat{\mathrm{v}}_0)}} \qquad (83)$$

Usually

$$\mathrm{f}_a = \mathrm{f}_0 = \mathrm{f}_b \qquad (84)$$

so that

$$m(\mathrm{f}_a, \mathrm{v}_0) e^{i \hat{m}(\mathrm{f}_b, \hat{\mathrm{v}}_0)} =$$

$$= m(\mathrm{f}_0, \mathrm{v}_0) e^{i \hat{m}(\mathrm{f}_0, \hat{\mathrm{v}}_0)} \equiv$$

$$\equiv \dot{m}(\mathrm{f}_0, \dot{\mathrm{v}}_0) \equiv \dot{\mathrm{m}}_0 \qquad (85)$$

and finally

$$\dot{k}(\mathrm{f}) \equiv \left(\frac{1}{\dot{\mathrm{m}}_0}\right) \dot{m}(\mathrm{f}, \dot{\mathrm{v}}_0) \qquad (86)$$

As before, we also assume linearity in the second complex variable and in this way, for the complex frequency response [8]

$$\forall\, \mathrm{f} \in \mathbf{f},\ \forall\, \dot{\mathrm{v}} \in \dot{\mathbf{v}},\ \exists!\, \dot{\mathrm{m}} \in \dot{\mathbb{m}},$$

$$\dot{\mathrm{m}} = \dot{m}(\mathrm{f}, \dot{\mathrm{v}}) = \dot{m}\left(\mathrm{f}, \dot{\mathrm{v}}\left(\frac{\dot{\mathrm{v}}_0}{\dot{\mathrm{v}}_0}\right)\right) = \ldots$$

$$= \left(\frac{\dot{\mathrm{m}}_0}{\dot{\mathrm{v}}_0}\right) \dot{k}(\mathrm{f}) \dot{\mathrm{v}} \qquad (87)$$

$$\dot{\boldsymbol{\alpha}} : \mathbf{f} \to \dot{\mathbb{C}};\ \forall\, \mathrm{f} \in \mathbf{f},\ \exists!\, \dot{\alpha} \in \dot{\mathbb{C}},$$

$$\dot{\alpha} = \dot{\alpha}(\mathrm{f}) \equiv \left(\frac{\dot{\mathrm{m}}_0}{\dot{\mathrm{v}}_0}\right) \dot{k}(\mathrm{f}) \qquad (88)$$

$$\boxed{\dot{\mathrm{m}} = \dot{m}(\mathrm{f}, \dot{\mathrm{v}}) = \dot{\alpha}(\mathrm{f}) \dot{\mathrm{v}}} \qquad (89)$$

B. The DUT

If Z_0 is the common real value of the characteristic impedance for the totality of the involved devices and we intend to measure only passive DUTs then the set of all possible reflection coefficients values $\dot{\rho}$ [9] is

$$\dot{\boldsymbol{\rho}} \equiv \{\dot{\rho} \mid 0 \leq |\dot{\rho}| \leq 1 \subset \dot{\mathbb{C}} \qquad (90)$$

$$\dot{\boldsymbol{\rho}}_{\mathbf{t}} : \mathbf{f} \to \dot{\boldsymbol{\rho}};\ \dot{\rho}_t \equiv \rho_t(\mathrm{f})$$

Geometrically, the sets $\dot{\mathbf{V}}_G$, $\dot{\mathbf{V}}_A$, $\dot{\mathbf{V}}_R$ and $\dot{\mathbb{m}}$ are annuluses around the origin O of the $\dot{\mathbb{C}}$ plane, the set $\dot{\boldsymbol{\rho}}$ is the unit circle with center at O and the sets $\mathbf{M_A}$ and $\mathbf{M_R}$ are segments of the positive real axis $\mathbb{R}_+$.The shape of the defined sets is shown in Fig. 4.

C. The IE

C1. The operation

We attempt to describe the IE operation by considering (Fig. 2) that the stimulus signal $\dot{\mathrm{v}}_g$ at the IE input port G in the presence of the DUT's $\dot{\rho}$ at IE port T, causes a pair of signals $\dot{\mathrm{v}}_a$ and $\dot{\mathrm{v}}_r$ to arise at the IE output ports A and R respectively. Obviously

$$\dot{\mathbf{v}}_{\mathbf{g}} \subseteq \dot{\mathbf{V}}_{\mathbf{0}} \qquad (91)$$

and furthermore we accept that the IE operation is described by a pair of smooth functions

$$\dot{\boldsymbol{v}}_{\mathbf{a}} : \dot{\boldsymbol{\rho}} \times \dot{\mathbf{v}}_{\mathbf{g}} \to \dot{\mathbf{V}}_{\mathbf{A}} \qquad (92)$$

$$\dot{\boldsymbol{v}}_{\mathbf{r}} : \dot{\boldsymbol{\rho}} \times \dot{\mathbf{v}}_{\mathbf{g}} \to \dot{\mathbf{V}}_{\mathbf{R}} \qquad \{93\}$$

and to avoid unnecessary complications between the produced and allowable voltage levels, we can accept that

$$\dot{\boldsymbol{v}}_{\mathbf{a}}[\dot{\boldsymbol{\rho}} \times \dot{\mathbf{v}}_{\mathbf{G}}] = \dot{\mathbf{v}}_{\mathbf{a}} \subseteq \dot{\mathbf{V}}_{\mathbf{A}} \text{ and} \qquad (94)$$

$$\dot{\boldsymbol{v}}_{\mathbf{r}}[\dot{\boldsymbol{\rho}} \times \dot{\mathbf{v}}_{\mathbf{G}}] = \dot{\mathbf{v}}_{\mathbf{r}} \subseteq \dot{\mathbf{V}}_{\mathbf{R}} \qquad (95)$$

In this way we have for the VNA signals

$$\dot{\mathrm{V}}_G = \dot{\mathrm{v}}_G,\ \dot{\mathrm{V}}_A = \dot{\mathrm{v}}_a,\ \dot{\mathrm{V}}_R = \dot{\mathrm{v}}_r,$$

$$\dot{\mathrm{v}} = \frac{\dot{\mathrm{V}}_A}{\dot{\mathrm{V}}_R} = \frac{\dot{\mathrm{v}}_a}{\dot{\mathrm{v}}_r} \qquad (96)$$

The IE can be viewed as a four port junction represented by the flow graph of Fig. 5 and described by the S-parameter matrix:

$$[\dot{\mathrm{S}}] = \begin{bmatrix} \dot{\mathrm{S}}_{GG} & \vdots & \dot{\mathrm{S}}_{GA} & \vdots & \dot{\mathrm{S}}_{GR} & \vdots & \dot{\mathrm{S}}_{GT} \\ \cdots & \vdots & \cdots & \vdots & \cdots & \vdots & \cdots \\ \dot{\mathrm{S}}_{AG} & \vdots & \dot{\mathrm{S}}_{AA} & \vdots & \dot{\mathrm{S}}_{AR} & \vdots & \dot{\mathrm{S}}_{AT} \\ \cdots & \vdots & \cdots & \vdots & \cdots & \vdots & \cdots \\ \dot{\mathrm{S}}_{RG} & \vdots & \dot{\mathrm{S}}_{RA} & \vdots & \dot{\mathrm{S}}_{RR} & \vdots & \dot{\mathrm{S}}_{RT} \\ \cdots & \vdots & \cdots & \vdots & \cdots & \vdots & \cdots \\ \dot{\mathrm{S}}_{TG} & \vdots & \dot{\mathrm{S}}_{TA} & \vdots & \dot{\mathrm{S}}_{TR} & \vdots & \dot{\mathrm{S}}_{TT} \end{bmatrix} \qquad (97)$$

If we shall use the wave-voltage signal equations in the only one propagated TEM mode at the frequency f then: If

$$\dot{\alpha}_x, \dot{\beta}_x \text{ and } \dot{a}_x, \dot{b}_x \qquad (98)$$

are the levels of the incoming and outgoing voltage waves at port

$$x = g, a, r, t, G, A, R, T \qquad (99)$$

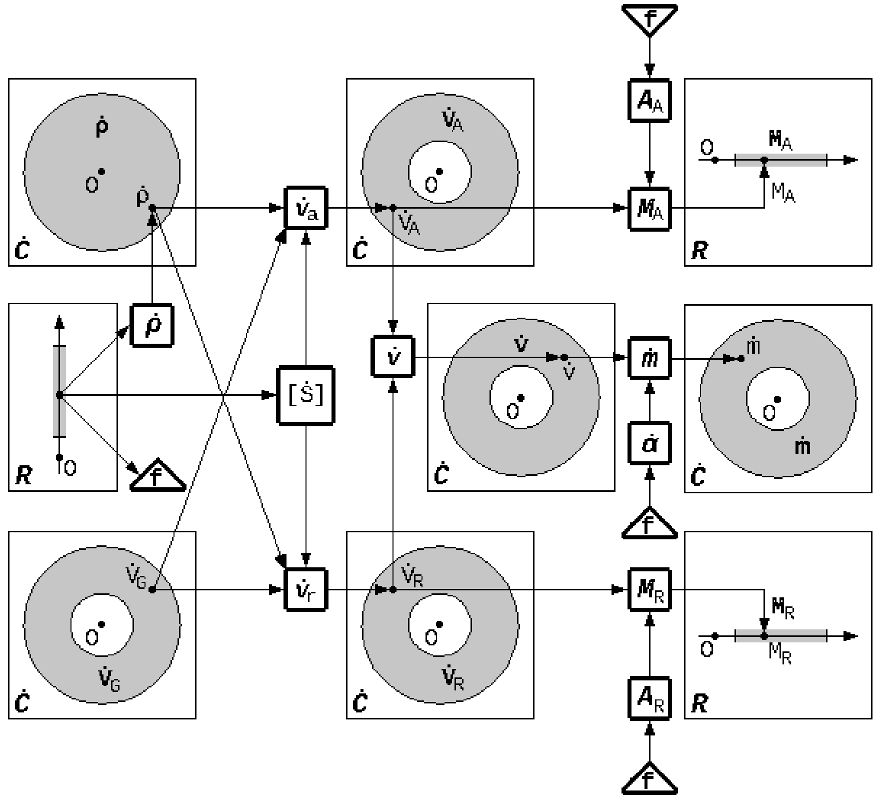

Fig. 4: The sets $\dot{\mathbf{V}}_G, \mathbf{f}, \dot{\boldsymbol{\rho}}, \dot{\mathbf{V}}_A, \dot{\mathbf{V}}_R, \dot{\mathbf{v}}, \dot{\mathrm{m}}, \mathbf{M_A}, \mathbf{M_R}$

of the VNA and IE respectively, as in (3) above, we have in vector-one column matrix notation:

$$[\dot{\alpha}] \equiv \bar{\alpha} = \bar{b} \equiv [\dot{b}] \qquad (100a)$$

$$[\dot{\beta}] \equiv \bar{\beta} = \bar{a} \equiv [\dot{a}] \qquad (100b)$$

$$\dot{V}_x = (\dot{\beta}_x + \dot{\alpha}_x)\sqrt{Z_0} = (\dot{a}_x + \dot{b}_x)\sqrt{Z_0} \qquad (101)$$

$$[\dot{\beta}] = [\dot{S}][\dot{\alpha}] \qquad (102)$$

$$[\dot{a}] = [\dot{S}][\dot{b}] \qquad (103)$$

but at each one of the ports we have the conditions

$$\dot{b}_G = \dot{\rho}_G \dot{a}_G + \dot{e}_G \qquad (104a)$$

$$\dot{b}_A = \dot{\rho}_A \dot{a}_A \qquad (104b)$$

$$\dot{b}_R = \dot{\rho}_R \dot{a}_R \qquad (104c)$$

$$\dot{b}_T = \dot{\rho}_T \dot{a}_T \qquad (104d)$$

or in matrix form

$$[\dot{b}] = [\dot{\rho}]^t [\mathrm{I}][\dot{a}] + [\dot{e}] \qquad (105)$$

and if $[\dot{S}]^{-1} \neq 0$ then (106)

$$[\dot{S}]^{-1}[\dot{a}] = [\dot{\rho}]^t[\mathrm{I}][\dot{a}] + [\dot{e}] \qquad (107)$$

$$([\dot{S}]^{-1} - [\dot{\rho}]^t[\mathrm{I}])[\dot{a}] = [\dot{e}] \qquad (108)$$

$$[\dot{\tilde{S}}] \equiv ([\dot{S}]^{-1} - [\dot{\rho}]^t[\mathrm{I}]) \qquad (109)$$

$$\dot{v} = \frac{\dot{V}_A}{\dot{V}_R} = \frac{\sqrt{Z_0}(\dot{a}_A + \dot{b}_A)}{\sqrt{Z_0}(\dot{a}_R + \dot{b}_R)} =$$

$$= \left(\frac{1 + \dot{\rho}_A}{1 + \dot{\rho}_R}\right)\left(\frac{\dot{a}_A}{\dot{a}_R}\right) = \dot{\sigma}\left(\frac{\dot{a}_A}{\dot{a}_R}\right) \qquad (110)$$

$$\dot{\sigma} \equiv \left(\frac{1 + \dot{\rho}_A}{1 + \dot{\rho}_R}\right) \qquad (111)$$

$$\frac{\dot{a}_A}{\dot{a}_R} = -\frac{|[\dot{\tilde{S}}_{GA}]|}{|[\dot{\tilde{S}}_{GR}]|} = \frac{-|[\dot{\tilde{S}}_{GA}]_{TG}|\,\dot{\tilde{S}}_{TG} + |[\dot{\tilde{S}}_{GA}]_{TR}|\,\dot{\tilde{S}}_{TR} - |[\dot{\tilde{S}}_{GA}]_{TT}|\,\dot{\tilde{S}}_{TT}}{|[\dot{\tilde{S}}_{GR}]_{TG}|\,\dot{\tilde{S}}_{TG} - |[\dot{\tilde{S}}_{GR}]_{TA}|\,\dot{\tilde{S}}_{TA} + |[\dot{\tilde{S}}_{GR}]_{TT}|\,\dot{\tilde{S}}_{TT}} =$$

$$= \frac{(-|[\dot{\tilde{S}}_{GA}]_{TG}|\,\dot{\tilde{S}}_{TG} + |[\dot{\tilde{S}}_{GA}]_{TR}|\,\dot{\tilde{S}}_{TR} - |[\dot{\tilde{S}}_{GA}]_{TT}|\,\dot{S}_{TT}^{-1}) + |[\dot{\tilde{S}}_{GA}]_{TT}|\,\dot{\rho}_T}{(|[\dot{\tilde{S}}_{GR}]_{TG}|\,\dot{\tilde{S}}_{TG} - |[\dot{\tilde{S}}_{GR}]_{TA}|\,\dot{\tilde{S}}_{TA} + |[\dot{\tilde{S}}_{GR}]_{TT}|\,\dot{S}_{TT}^{-1}) - |[\dot{\tilde{S}}_{GR}]_{TT}|\,\dot{\rho}_T} \qquad (112)$$

Setting

$$\dot{A} \equiv |[\dot{\tilde{S}}_{GA}]_{TT}| \qquad (113)$$

$$\dot{B} \equiv (-|[\dot{\tilde{S}}_{GA}]_{TG}|\,\dot{\tilde{S}}_{TG} + |[\dot{\tilde{S}}_{GA}]_{TR}|\,\dot{\tilde{S}}_{TR} - |[\dot{\tilde{S}}_{GA}]_{TT}|\,\dot{S}_{TT}^{-1}) \qquad (114)$$

$$\dot{\Gamma} \equiv -|[\dot{\tilde{S}}_{GR}]_{TT}| \qquad (115)$$

$$\dot{\Delta} \equiv (|[\dot{\tilde{S}}_{GR}]_{TG}|\,\dot{\tilde{S}}_{TG} - |[\dot{\tilde{S}}_{GR}]_{TA}|\,\dot{\tilde{S}}_{TA} + |[\dot{\tilde{S}}_{GR}]_{TT}|\,\dot{S}_{TT}^{-1}) \qquad (116)$$

then from (110) and (111)

$$\dot{v} = \dot{\sigma}\left(\frac{\dot{A}\dot{\rho} + \dot{B}}{\dot{\Gamma}\dot{\rho} + \dot{\Delta}}\right) = \frac{(\dot{\sigma}\dot{A})\dot{\rho} + (\dot{\sigma}\dot{B})}{(\dot{\Gamma})\dot{\rho} + (\dot{\Delta})} \qquad (117)$$

and from (89) the measurement $\dot{m}$ is given by

$$\dot{m} = \dot{m}(f, \dot{v}) = \dot{\alpha}(f)\dot{v} = \dot{\alpha}(f)\dot{\sigma}\left(\frac{\dot{a}_A}{\dot{a}_R}\right) =$$

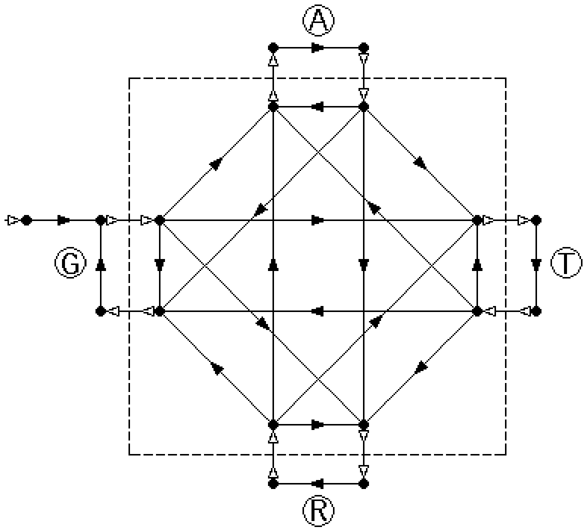

Fig. 5: The four port junction flow graph of the IE

$$= \dot\alpha(f)\dot\sigma\left(\frac{\dot A\dot\rho + \dot B}{\dot\Gamma\dot\rho + \dot\Delta}\right) \qquad (118)$$

Error Parameters Formulation

It is given [1] that in network analyzer measurements with one port error model are involved initially five complex quantities, named as

$\dot\rho$ for the reflection coefficient of the unknown load,

$\dot m$ for its measured value,

$\dot D$ for the directivity error,

$\dot M$ for the source match error and

$\dot R$ for the frequency response error which equals to $(1+\dot T)$, where $\dot T$ stands for the reflection tracking error.

The above quantities are shown in the well known flow graph of Fig. 6 [10], [11] and verify the relation

$$\dot m = \dot D + \frac{\dot R\dot\rho}{1-\dot M\dot\rho} \qquad (119)$$

which is the starting point of our discussion and with a re-arrangement becomes

$$\dot m = \frac{(\dot R - \dot D\dot M)\dot\rho + (\dot D)}{(-\dot M)\dot\rho + (1)} \qquad (120)$$

and from (118)

$$\dot m = \frac{\left(\frac{\dot\alpha(f)\dot\sigma\dot A}{\dot\Delta}\right)\dot\rho + \left(\frac{\dot\alpha(f)\dot\sigma\dot B}{\dot\Delta}\right)}{\left(\frac{\dot\Gamma}{\dot\Delta}\right)\dot\rho + (1)} \qquad (121)$$

where

$$\dot M \equiv -\left(\frac{\dot\Gamma}{\dot\Delta}\right) \qquad (122a)$$

$$\dot D \equiv \left(\frac{\dot\alpha(f)\dot\sigma\dot B}{\dot\Delta}\right) \qquad (122b)$$

$$\dot R \equiv \left(\frac{\dot\alpha(f)\dot\sigma\dot A}{\dot\Delta}\right) - \left(\frac{\dot\Gamma}{\dot\Delta}\right)\left(\frac{\dot\alpha(f)\dot\sigma\dot B}{\dot\Delta}\right) \qquad (122c)$$

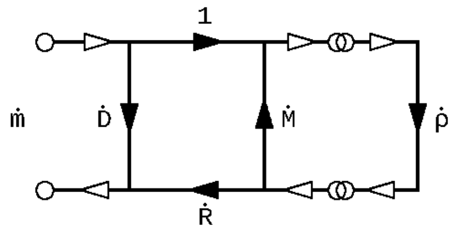

Fig. 6: One port error model

We are interested of course to compute $\dot\rho$, hence by (119), we have

$$\dot\rho = \frac{\dot m - \dot D}{\dot M(\dot m - \dot D) + \dot R} \qquad (123a)$$

and in as a typically bilinear function form [2]

$$\dot\rho = \frac{(1)\dot m + (-\dot D)}{(\dot M)\dot m + (\dot R - \dot M\dot D)} \qquad (123b)$$

which is characterized by the constants 1, $-\dot D$, $\dot M$, $\dot R - \dot M\dot D$ or by defining

$$\dot Q \equiv \dot R - \dot M\dot D \qquad (124)$$

we take finally

$$\dot\rho = \frac{\dot m - \dot D}{\dot M\dot m + \dot Q} \qquad (125)$$

By re-arranging the terms of (125) we take in array-vector form

$$\left[\dot\rho \;\vdots\; \dot\rho\dot m \;\vdots\; 1\right]\begin{bmatrix}\dot Q\\ \cdots\\ \dot M\\ \cdots\\ \dot D\end{bmatrix} = \dot m \qquad (126)$$

We find the constants of the bilinear transformation by applying the "One Port Full Calibration Method" [1] and defining Standard Loads $\dot S$, $\dot L$, $\dot O$, and their respective measurements $\dot s$, $\dot l$, $\dot o$, as follows

$\dot S, \dot s$: for "Shortcircuit" with typical value –1,

$\dot L$, $\dot l$: for "matching Load", tyically 0 and

$\dot O$, $\dot o$: for "Opencircuit", typically 1.

We have from (126) in matrix form

$$\begin{bmatrix}\dot O & \vdots & \dot O\dot o & \vdots & 1\\ \cdots & & \cdots & & \cdots\\ \dot S & \vdots & \dot S\dot s & \vdots & 1\\ \cdots & & \cdots & & \cdots\\ \dot L & \vdots & \dot L\dot l & \vdots & 1\end{bmatrix}\begin{bmatrix}\dot Q\\ \cdots\\ \dot M\\ \cdots\\ \dot D\end{bmatrix} = \left[\dot o \;\vdots\; \dot s \;\vdots\; \dot l\right] \qquad (127)$$

We define as

$$\dot{A} \equiv \begin{bmatrix} \dot{O} & \vdots & \dot{O}\dot{o} & \vdots & 1 \\ \cdots & & \cdots & & \cdots \\ \dot{S} & \vdots & \dot{S}\dot{s} & \vdots & 1 \\ \cdots & & \cdots & & \cdots \\ \dot{L} & \vdots & \dot{L}\dot{l} & \vdots & 1 \end{bmatrix} \tag{128}$$

The determinant of $\dot{A}$ is

$$\begin{aligned}[\dot{A}] = \dot{O}(\dot{L}-\dot{S})\dot{o} + \dot{S}(\dot{O}-\dot{L})\dot{s} + \\ + \dot{L}(\dot{S}-\dot{O})\dot{l}\end{aligned} \tag{129}$$

At this point we note that the manipulation of the rather lengthy expressions is greatly facilitated by the observation of the cyclic nature of the forms over the letters S,L,O and s,l,o respectively. By the introduction of the symbol $\sum\limits_{\circ}$ for the cyclic summation we have [11]

$$\boxed{[\dot{A}] = \sum_{\circ} \dot{o}\dot{O}(\dot{L}-\dot{S})} \tag{130}$$

The inverse of $\dot{A}$ is

$$\dot{A}^{-1} = \begin{bmatrix} \dot{O} & \vdots & \dot{O}\dot{o} & \vdots & 1 \\ \cdots & & \cdots & & \cdots \\ \dot{S} & \vdots & \dot{S}\dot{s} & \vdots & 1 \\ \cdots & & \cdots & & \cdots \\ \dot{L} & \vdots & \dot{L}\dot{l} & \vdots & 1 \end{bmatrix}^{-1} = \frac{1}{[\dot{A}]} \begin{bmatrix} \dot{S}\dot{s}-\dot{L}\dot{l} & \vdots & \dot{L}\dot{l}-\dot{O}\dot{o} & \vdots & \dot{O}\dot{o}-\dot{S}\dot{s} \\ \cdots & & \cdots & & \cdots \\ \dot{L}-\dot{S} & \vdots & \dot{O}-\dot{L} & \vdots & \dot{S}-\dot{O} \\ \cdots & & \cdots & & \cdots \\ \dot{S}\dot{L}(\dot{l}-\dot{s}) & \vdots & \dot{O}\dot{L}(\dot{o}-\dot{l}) & \vdots & \dot{O}\dot{S}(\dot{s}-\dot{o}) \end{bmatrix} \tag{131}$$

and the solution of the system is

$$\begin{bmatrix} \dot{Q} \\ \cdots \\ \dot{M} \\ \cdots \\ \dot{D} \end{bmatrix} = \frac{1}{[\dot{A}]} \begin{bmatrix} \dot{S}\dot{s}-\dot{L}\dot{l} & \vdots & \dot{L}\dot{l}-\dot{O}\dot{o} & \vdots & \dot{O}\dot{o}-\dot{S}\dot{s} \\ \cdots & & \cdots & & \cdots \\ \dot{L}-\dot{S} & \vdots & \dot{O}-\dot{L} & \vdots & \dot{S}-\dot{O} \\ \cdots & & \cdots & & \cdots \\ \dot{S}\dot{L}(\dot{l}-\dot{s}) & \vdots & \dot{O}\dot{L}(\dot{o}-\dot{l}) & \vdots & \dot{O}\dot{S}(\dot{s}-\dot{o}) \end{bmatrix} \begin{bmatrix} \dot{o} \\ \cdots \\ \dot{s} \\ \cdots \\ \dot{l} \end{bmatrix} \tag{132}$$

or in the cyclic form

$$\dot{Q} = \frac{1}{[\dot{A}]} \sum_{\circ} \dot{s}\dot{l}(\dot{L}-\dot{S}) \tag{133}$$

$$\dot{M} = \frac{1}{[\dot{A}]} \sum_{\circ} \dot{o}(\dot{L}-\dot{S}) \tag{134}$$

$$\dot{D} = -\frac{1}{[\dot{A}]} \sum_{\circ} \dot{s}\dot{l}\dot{O}(\dot{L}-\dot{S}) \tag{135}$$

$$\dot{R} = \frac{1}{[\dot{A}]} \prod_{\circ} (\dot{S}-\dot{L})(\dot{s}-\dot{l}) \tag{136}$$

and thus (125) becomes [12]

$$\dot{\rho} = \frac{\dot{S}(\dot{L}-\dot{O})(\dot{m}\dot{s}+\dot{l}\dot{o}) + \dot{L}(\dot{O}-\dot{S})(\dot{m}\dot{l}+\dot{o}\dot{s}) + \dot{O}(\dot{S}-\dot{L})(\dot{m}\dot{o}+\dot{s}\dot{l})}{(\dot{L}-\dot{O})(\dot{m}\dot{s}+\dot{l}\dot{o}) + (\dot{O}-\dot{S})(\dot{m}\dot{l}+\dot{o}\dot{s}) + (\dot{S}-\dot{L})(\dot{m}\dot{o}+\dot{s}\dot{l})} \tag{137}$$

In the measurement system in use, the "other support devices" of Fig. 2 included mainly a Phase Locked arrangement with 100Hz step signal generator, a 10-digits frequency counter ([13] - [15]) and a personal computer which runs developed by us (therefore completely manageable) software in IEEE-488 for the device control, in Visual Basic for the data collection and in Mathematica for the data processing ([16] – [22]).

Practical Applications

The VNA characteristics as sets of values are given in [23] - [25]. Tab. 1 gives only those characteristics that are clearly stated and related exclusively to reflection measurements. Tab. 2 contains some of the performance tests that were performed and again are related only to the reflection measurements [26]. The HP909A male standard load was used as matching load.

To construct the $\boldsymbol{\dot{v}}$ function, with its value $\dot{v}$ to be given through (110) we start from a given circuit diagram for the T/R Test Set [26]. In Fig. 7 we have simplified this circuit along with the IE's transmission lines (TLs).

In the equivalent circuit which is actually an RF simplification of the original, we have omitted:

(i) The bias circuitry (input connector, feed-through capacitor, RF chock and all the other blocking capacitors), and

(ii) The step attenuator and its corresponding electrical length compensation transmission line segments, because we do not use them. On the other hand we have assumed properly formed values for the resistors of the pad. In the circuit of Fig. 7 are readily recognized.

It is obvious that the rest of the elements can be thought as they form a power divider - directional bridge combination supported by the compensation pad and by the isolation transformer with a detail note that the pad’s resistor values are taken by implication based on the rest of the circuit characteristics. Our study is limited by the extent of our knowledge about the characteristics of the various devices involved. In order to clear once at all the role-played by the T/R Test Set in forming the relation between $\dot{m}$, $\dot{Z}$ we analyze its equivalent circuit as it is shown in Fig. 8.

Tab. 1: VNA characteristics for reflection measurements

$\widetilde{\mathbf{P}}_0$ [dBm]	−72 - +10
Input Level [dBm]	−10 or −30
f [MHz]	0.5 - 1300
Dynamic Range $\widetilde{\mathbf{M}}_i$[dBm]	−110 - −10
Dynamic Range **v** [dB]	100
$\mathbf{M}_i$ [dB]	−199.99 - +199.99
Magnitude HPIB [dB]	xxx.xx
Phase [°]	−180 - +180
Phase HPIB [°]	xxxx.x

Tab. 2: Performance test record for reflection measurements

Description	Lower Limit	Measured Value	Upper Limit
Directivity [dB]	40	43.3	
Transmission Frequency Response			
MAG [dB]:		0.7	0.8
PHASE [°]:		5	8
Reflection Frequency Response			
MAG [dB]: 0.5 - 1300 MHz		0.4	1.5
PHASE [°]: 0.5 - 1300 MHz		2.5	15
PHASE [°]: 2 - 1300 MHz		2	10
Test Port Open/Short Ratio			
MAG [dB]: 1000 - 1300 MHz		0.54	1.8
PHASE [°]: 1000 - 1300 MHz		8	15
MAG [dB]: 2 - 1300 MHz		0.3	1.5
PHASE [°]: 2 - 1300 MHz		6.5	12
MAG [dB]: 0.5 - 2 MHz		1.9	2.5
PHASE [°]: 0.5 - 2 MHz		5.6	20

Description	Lower	Measured	Upper
Magnitude Reference Offset and Marker Accuracy Test			
Rectangular marker Zero [dB]	−0.01	0.00	+0.01
Polar Marker Zero - Magnitude of Outside circle	−3 mm	0	+3 mm
Polar marker Zero - Phase [°]	−1	0	+1
Offset +190 dB & read marker	−184	−190.1	−196
Offset −190 dB & read marker	+184	+190	+196
Crosstalk Isolation [dB]			
Crosstalk between R and A Port	100	−117.3	
Crosstalk between A and R Port	100	−119.2	
Magnitude and Phase Frequency Response			
Port R [dB]		2	3
Port A [dB]		2	3
A/R Ratio Magnitude [dB]		0.47	0.6
A/R Ratio Phase [°]:			
0.5 - 750 MHz		6	6
750 – 1300 MHz		4	10
Phase Reference Offset			
Reference Offset, CRT trace tolerance from reference line:			
±360°	−2.1	0.8	+2.1
±720°	−3.9	1.5	+3.9
±1080°	−5.7	2.0	+5.7
±1440°	−7.0	2.6	+7.5
Phase Accuracy Test			
+180° transition	+182	181	+178
−180° transition	−182	−180	−178
Input Impedance Test			
Return Loss of Port A [dB]	20	−25	
Return Loss of Port R [dB]	20	−23	
Source Impedance Test			
SWR of RF OUTPUT port		1.15	1.38

Indices for ports are as page oriented: L-R-U-D (Left, Right, Up, Down). The S-parameter matrix

$$[\dot{S}^X] = \begin{bmatrix} \dot{S}^X_{ii} & \vdots & \dot{S}^X_{ij} \\ \cdots & \vdots & \cdots \\ \dot{S}^X_{ji} & \vdots & \dot{S}^X_{jj} \end{bmatrix} =$$

$$= \begin{bmatrix} 0 & \vdots & e^{-\dot{\gamma}^X L^X} \\ \cdots & \vdots & \cdots \\ e^{-\dot{\gamma}^X L^X} & \vdots & 0 \end{bmatrix} \qquad (138)$$

stands for the IE's transmission lines, where

X = H, I, J, K

$\dot{\gamma}$ is the well known propagation factor $\alpha + i\beta$

L is the length of the line.

The transformer F can be described by the matrix

$$[\dot{S}^F] = \begin{bmatrix} \dot{S}^F_{ll} & \vdots & \dot{S}^F_{lr} \\ \cdots & \vdots & \cdots \\ \dot{S}^F_{rl} & \vdots & \dot{S}^F_{rr} \end{bmatrix} = \begin{bmatrix} 0 & \vdots & 1 \\ \cdots & \vdots & \cdots \\ 1 & \vdots & 0 \end{bmatrix} \qquad (139)$$

The compensation pad C

$$[\dot{S}^C] = \begin{bmatrix} \dot{S}^C_{dd} & \vdots & \dot{S}^C_{du} \\ \cdots & \vdots & \cdots \\ \dot{S}^C_{ud} & \vdots & \dot{S}^F_{uu} \end{bmatrix} = \begin{bmatrix} 0 & \vdots & \frac{1}{4} \\ \cdots & \vdots & \cdots \\ \frac{1}{4} & \vdots & 0 \end{bmatrix} \qquad (140)$$

The power divider P by matrix (141) and the directional bridge B by matrix (142).

Now that we know the S-parameters of all the components parts of the T/R Set circuit (Fig. 7) we can use the flow graph techniques-rules [27], [28] and the topology of the graph of Fig. 8 to determine the S-parameters of the equivalent four port (Fig. 5) and by means of them to express $\dot{v}$ and finally $\dot{m}$. Thus we obtain the matrix (143) for the $[\dot{S}]$ matrix of (97).

In the most simplified case where the transmission lines H, I, J and K are substituted by ideal connectors which implies that the secondary diagonal elements of $[\dot{S}^X]$ matrices are unitary, the $[\dot{S}]$ matrix becomes real (144).

In order to illustrate the above result we redraw Fig. 5 and obtain Fig. 9. From (144), (110) and Fig. 9, and since $\dot{\sigma} = 1$ for matched ports A, R with $\dot{\rho}_A = 0 = \dot{\rho}_R$, we have for $\dot{v}$

$$\frac{\dot{a}_A}{\dot{a}_R} = \frac{\dot{S}_{AG} + (\dot{S}_{AT}\dot{S}_{TG} - \dot{S}_{TT}\dot{S}_{AG})\dot{\rho}}{\dot{S}_{RG} + (\dot{S}_{RT}\dot{S}_{TG} - \dot{S}_{TT}\dot{S}_{RG})\dot{\rho}} =$$

$$= \frac{0 + (\frac{1}{2} \times \frac{1}{4} - \frac{1}{16} 0)\dot{\rho}}{\frac{1}{8} + (\frac{1}{32} \times \frac{1}{4} - \frac{1}{16} \times \frac{1}{8})\dot{\rho}} =$$

$$= \frac{\frac{1}{8}\dot{\rho}}{\frac{1}{8}} = \dot{\rho} \qquad (145)$$

as we expected for this ideal case.

If we return to the most general case which indicates the existence of the H, I, J, K different transmission lines then the $[\dot{S}]$ matrix and the above ratio of the incoming voltage waves at A and R ports of the VNA we take the expressions (146) and (147) respectively.

$$[\dot{S}^P] = \begin{bmatrix} \dot{S}^P_{ll} & \vdots & \dot{S}^P_{lu} & \vdots & \dot{S}^P_{lr} \\ \cdots & \vdots & \cdots & \vdots & \cdots \\ \dot{S}^P_{ul} & \vdots & \dot{S}^P_{uu} & \vdots & \dot{S}^P_{ur} \\ \cdots & \vdots & \cdots & \vdots & \cdots \\ \dot{S}^P_{rl} & \vdots & \dot{S}^P_{ru} & \vdots & \dot{S}^P_{rr} \end{bmatrix} = \frac{1}{3 + \dot{\zeta}} \begin{bmatrix} \dot{\zeta} - 1 & \vdots & 2 & \vdots & 2 \\ \cdots & \vdots & \cdots & \vdots & \cdots \\ 2 & \vdots & \frac{(1+\dot{\zeta})^2 - 2}{1+\dot{\zeta}} & \vdots & \frac{2}{1+\dot{\zeta}} \\ \cdots & \vdots & \cdots & \vdots & \cdots \\ 2 & \vdots & \frac{2}{1+\dot{\zeta}} & \vdots & \frac{(1+\dot{\zeta})^2 - 2}{1+\dot{\zeta}} \end{bmatrix}$$

$$= \begin{bmatrix} 0 & \vdots & \frac{1}{2} & \vdots & \frac{1}{2} \\ \cdots & \vdots & \cdots & \vdots & \cdots \\ \frac{1}{2} & \vdots & \frac{1}{4} & \vdots & \frac{1}{4} \\ \cdots & \vdots & \cdots & \vdots & \cdots \\ \frac{1}{2} & \vdots & \frac{1}{4} & \vdots & \frac{1}{4} \end{bmatrix} \qquad (141)$$

$$[\dot{S}^B] = \begin{bmatrix} \dot{S}^B_{ll} & \vdots & \dot{S}^B_{lu} & \vdots & \dot{S}^B_{lr} \\ \cdots & \vdots & \cdots & \vdots & \cdots \\ \dot{S}^B_{ul} & \vdots & \dot{S}^B_{uu} & \vdots & \dot{S}^B_{ur} \\ \cdots & \vdots & \cdots & \vdots & \cdots \\ \dot{S}^B_{rl} & \vdots & \dot{S}^B_{ru} & \vdots & \dot{S}^B_{rr} \end{bmatrix} = \begin{bmatrix} 0 & \vdots & 0 & \vdots & \frac{1}{2} \\ \cdots & \vdots & \cdots & \vdots & \cdots \\ 0 & \vdots & 0 & \vdots & \frac{1}{2} \\ \cdots & \vdots & \cdots & \vdots & \cdots \\ \frac{1}{2} & \vdots & \frac{1}{2} & \vdots & 0 \end{bmatrix} \qquad (142)$$

$$[\dot{S}] = \begin{bmatrix} 0 & \dot{S}^{J}_{du}\dot{S}^{B}_{lu}\dot{S}^{F}_{lr} * \dot{S}^{P}_{lr}\dot{S}^{H}_{lr} & \dot{S}^{I}_{du}\dot{S}^{C}_{du} * \dot{S}^{P}_{lu}\dot{S}^{H}_{lr} & \dot{S}^{K}_{lr}\dot{S}^{B}_{lr}\dot{S}^{F}_{lr} * \dot{S}^{P}_{lr}\dot{S}^{H}_{lr} \\ \cdots & \cdots & \cdots & \cdots \\ \dot{S}^{H}_{rl}\dot{S}^{P}_{rl}\dot{S}^{F}_{rl} * \dot{S}^{B}_{ul}\dot{S}^{J}_{ud} & 0 & \dot{S}^{I}_{du}\dot{S}^{C}_{du}\dot{S}^{P}_{ru} * \dot{S}^{F}_{rl}\dot{S}^{B}_{ur}\dot{S}^{J}_{ud} & \dot{S}^{K}_{lr}\dot{S}^{B}_{ur}\dot{S}^{J}_{ud} + \dot{S}^{K}_{lr}\dot{S}^{B}_{lr}\dot{S}^{F}_{lr} * \dot{S}^{P}_{rr}\dot{S}^{F}_{rl}\dot{S}^{B}_{ul}\dot{S}^{J}_{ud} \\ \cdots & \cdots & \cdots & \cdots \\ \dot{S}^{H}_{rl}\dot{S}^{P}_{ul} * \dot{S}^{C}_{ud}\dot{S}^{I}_{ud} & \dot{S}^{J}_{du}\dot{S}^{B}_{lu}\dot{S}^{F}_{lr} * \dot{S}^{P}_{ur}\dot{S}^{C}_{ud}\dot{S}^{I}_{ud} & \dot{S}^{I}_{du}\dot{S}^{C}_{du}\dot{S}^{P}_{uu} * \dot{S}^{C}_{ud}\dot{S}^{I}_{ud} & \dot{S}^{K}_{lr}\dot{S}^{B}_{lr}\dot{S}^{F}_{lr} * \dot{S}^{P}_{ur}\dot{S}^{C}_{ud}\dot{S}^{I}_{ud} \\ \cdots & \cdots & \cdots & \cdots \\ \dot{S}^{H}_{rl}\dot{S}^{P}_{rl}\dot{S}^{F}_{rl} * \dot{S}^{B}_{rl}\dot{S}^{K}_{rl} & \dot{S}^{J}_{du}\dot{S}^{B}_{ru}\dot{S}^{K}_{rl} & \dot{S}^{I}_{du}\dot{S}^{C}_{du}\dot{S}^{P}_{ru} * \dot{S}^{F}_{lr}\dot{S}^{B}_{rl}\dot{S}^{K}_{rl} & \dot{S}^{K}_{lr}\dot{S}^{B}_{lr}\dot{S}^{F}_{lr} * \dot{S}^{P}_{rr}\dot{S}^{F}_{rl}\dot{S}^{B}_{rl}\dot{S}^{K}_{rl} \end{bmatrix} \quad (143)$$

$$[\dot{S}] = \begin{bmatrix} 0 & 0 & \frac{1}{8} & \frac{1}{4} \\ \cdots & \cdots & \cdots & \cdots \\ 0 & 0 & 0 & \frac{1}{2} \\ \cdots & \cdots & \cdots & \cdots \\ \frac{1}{8} & 0 & \frac{1}{64} & \frac{1}{32} \\ \cdots & \cdots & \cdots & \cdots \\ \frac{1}{4} & \frac{1}{2} & \frac{1}{32} & \frac{1}{16} \end{bmatrix} \quad (144)$$

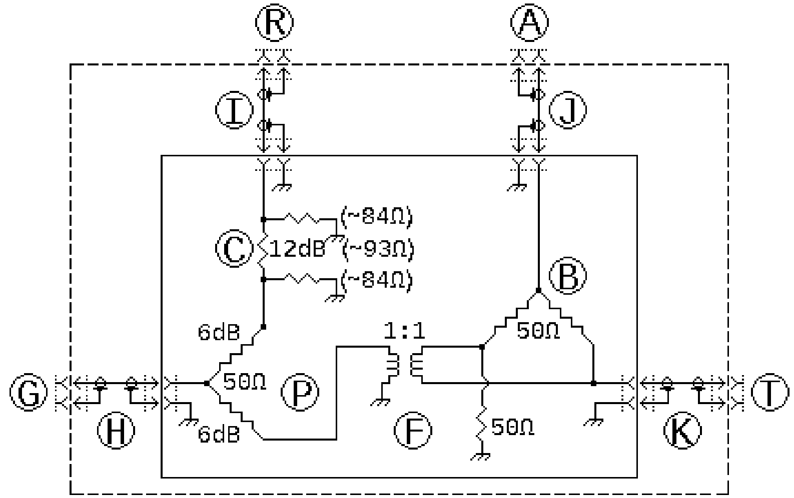

Fig. 7: Simplified T/R Test Set equivalent circuit

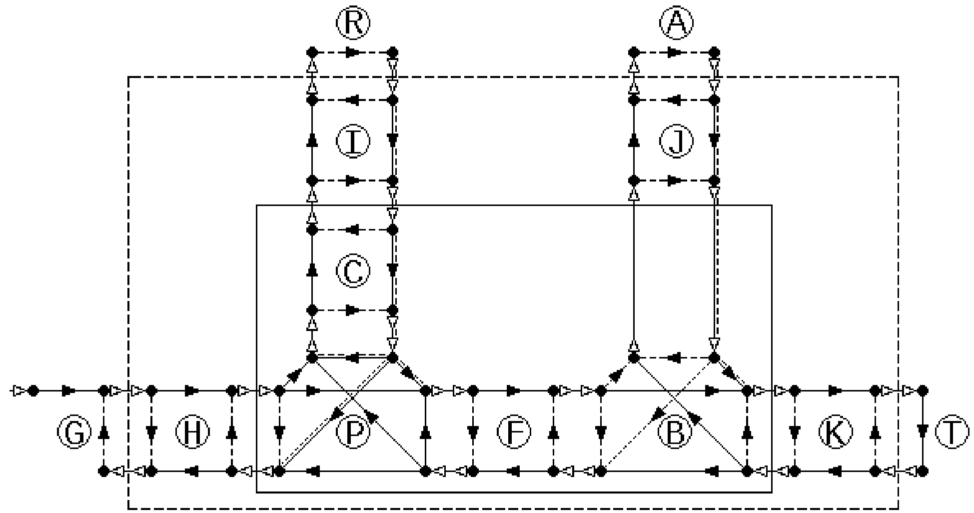

Fig. 8: Flow graph of the simplified T/R Test Set of Fig. 7

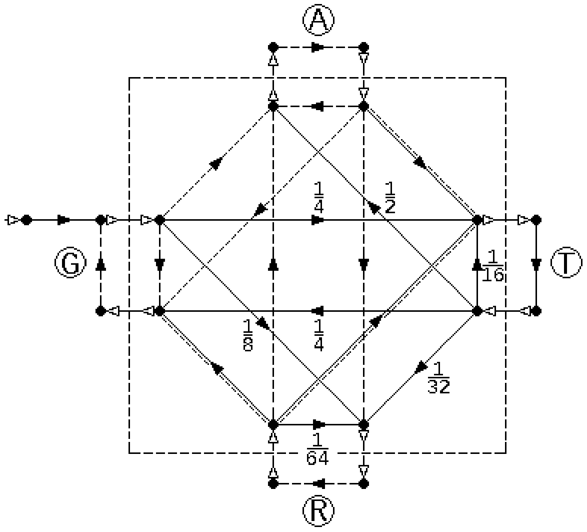

Fig. 9: The four port flow graph of the simplified IE

$$[\dot{S}]=\begin{bmatrix} 0 & 0 & \frac{1}{8}e^{-\dot{\gamma}^H L^H}e^{-\dot{\gamma}^I L^I} & \frac{1}{4}e^{-\dot{\gamma}^H L^H}e^{-\dot{\gamma}^K L^K} \\ \cdots & \cdots & \cdots & \cdots \\ 0 & 0 & 0 & \frac{1}{2}e^{-\dot{\gamma}^J L^J}e^{-\dot{\gamma}^K L^K} \\ \cdots & \cdots & \cdots & \cdots \\ \frac{1}{8}e^{-\dot{\gamma}^H L^H}e^{-\dot{\gamma}^I L^I} & 0 & \frac{1}{64}e^{-2\dot{\gamma}^I L^I} & \frac{1}{32}e^{-\dot{\gamma}^I L^I}e^{-\dot{\gamma}^K L^K} \\ \cdots & \cdots & \cdots & \cdots \\ \frac{1}{4}e^{-\dot{\gamma}^H L^H}e^{-\dot{\gamma}^K L^K} & \frac{1}{2}e^{-\dot{\gamma}^J L^J}e^{-\dot{\gamma}^K L^K} & \frac{1}{32}e^{-\dot{\gamma}^I L^I}e^{-\dot{\gamma}^K L^K} & \frac{1}{16}e^{-2\dot{\gamma}^K L^K} \end{bmatrix} \quad (146)$$

$$\frac{\dot{a}_A}{\dot{a}_R}=\frac{\dot{S}_{AG}+(\dot{S}_{AT}\dot{S}_{TG}-\dot{S}_{TT}\dot{S}_{AG})\dot{\rho}}{\dot{S}_{RG}+(\dot{S}_{RT}\dot{S}_{TG}-\dot{S}_{TT}\dot{S}_{RG})\dot{\rho}}=\frac{0+\dot{S}_{AT}\dot{S}_{TG}\dot{\rho}}{\dot{S}_{RG}+0\dot{\rho}}=\left(\frac{e^{-\dot{\gamma}^J L^J}}{e^{-\dot{\gamma}^I L^I}}\right)e^{-2\dot{\gamma}^K L^K}\dot{\rho}=\left(\frac{e^{-\dot{\gamma}^J L^J}}{e^{-\dot{\gamma}^I L^I}}\right)e^{-2\dot{\gamma}^K L^K}\dot{\rho} \quad (147)$$

And finally

$$\frac{\dot{a}_A}{\dot{a}_R}=e^{-2\dot{\gamma}^K L^K}\dot{\rho} \quad (148)$$

which concludes from the fact that the I, J transmission lines are identical in size and type.

A. Response Calibration

Response calibration means that instead of three Standard Loads we have only one available, the short circuit, which measurement is the reference for any other unknown load [29], [30]. As we mentioned before a typical value for this load is –1 and if for simplicity we assume that

$$\dot{\alpha}(f)\dot{\sigma}=1 \quad (149)$$

then (148) becomes

$$\dot{s}=e^{-2\dot{\gamma}^K L^K}\dot{\rho}=e^{-2\dot{\gamma}^K L^K}\dot{S}=-e^{-2\dot{\gamma}^K L^K} \quad (150)$$

Thus, for an unknown load

$$\dot{m}=e^{-2\dot{\gamma}^K L^K}\dot{\rho}=-\dot{s}\dot{\rho}\Rightarrow\dot{\rho}=-\frac{\dot{m}}{\dot{s}} \quad (151)$$

B. A typical measurement application

First we assume that the three Standard loads $\dot{S}$, $\dot{L}$, $\dot{O}$, for the calibration procedure posses their theoretical values ([31], [32])

$$\dot{S}=-1.0,\ \dot{L}=0.0,\ \dot{O}=1.0 \quad (152)$$

Thus, the quantities of (130), (134) - (137) are simplified as

$$[\dot{A}]=\dot{o}-\dot{s} \quad (153)$$

$$\dot{Q}=\frac{\dot{l}(\dot{o}+\dot{s})-2\dot{o}\dot{s}}{\dot{o}-\dot{s}} \quad (154)$$

$$\dot{D}=\dot{l} \quad (155)$$

$$\dot{M}=\frac{\dot{o}+\dot{s}-2\dot{l}}{\dot{o}-\dot{s}}g \quad (156)$$

$$\dot{R}=\frac{2(\dot{l}-\dot{o})(\dot{s}-\dot{l})}{\dot{o}-\dot{s}} \quad (157)$$

$$\boxed{\dot{\rho}=\frac{(\dot{m}-\dot{l})(\dot{o}-\dot{s})}{(\dot{m}-\dot{o})(\dot{s}-\dot{l})-(\dot{m}-\dot{s})(\dot{l}-\dot{o})}} \quad (158)$$

the ρ-mini expression for the reflection coefficient [12], which can be written in the bilinear form (159)

$$\dot{\rho}=\frac{\dot{m}(\dot{o}-\dot{s})+(-\dot{l}(\dot{o}-\dot{s}))}{\dot{m}(\dot{s}+\dot{o}-2\dot{l})+(\dot{l}(\dot{s}+\dot{o})-2\dot{s}\dot{o})}$$

In Fig.10 are illustrated the three error parameters $\dot{D}$, $\dot{M}$, $\dot{R}$ where they are given in plane as real, with single prime, and imaginary part with double prime and in space as functions of frequency for the range 550 MHz-1300 MHz. The VNA system used is fully described in [11] and [33] as the first system.

The automated measurements were taken by means of our program [ANALYZE] through HPIB/IEEE 488 [34].

Then we measured one of the 436 antenna models that were constructed [35] with the geometric model of Fig. 11, which is one of the four possible arrangements of a multi-frequency decoupling cylinder with one of the possible monopoles, here the conical one. Fig. 12 shows the simulation model with 16 wires for the cylinders and 8 wires for the conical monopole with dimensions: $d_1 = 8$cm, $L_1 = 9$cm, $d_2 = .9.6$cm $L_2 = 8$cm, $s = = 0.8$cm, $\alpha = = 90°$, $H = 6$cm. Full details of the construction are given in [35].

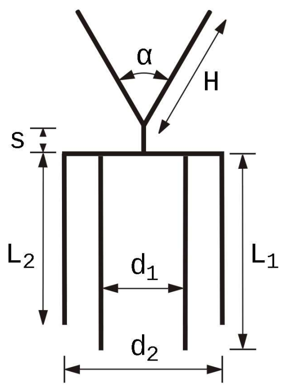

Fig. 11 Antenna geometry with down external step

The antenna's reflection coefficient after full one-port calibration with SLO (158) and after only response calibration S (151) is shown in plane and in space as function of frequency in Fig. 13 among with their comparison. In Fig. 14 the antenna's input impedance is illustrated as real and imaginary part together with their prediction from simulation by [RICHWIRE] [36], with the gray cloud to represent their measurements' DEIs (Differential Error Intervals) [11]. All the measurements were performed in the anechoic chamber of the Antennas Research Group when it was hosted by the university.

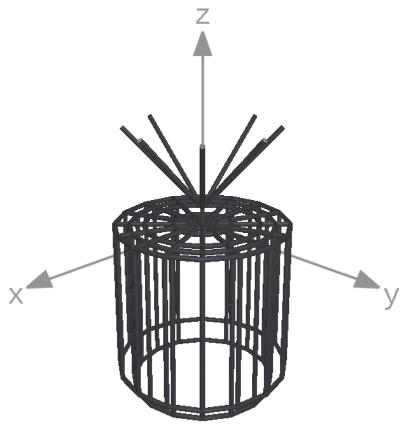

Fig. 12: Simulation model

The input impedance is given by the well known expression as function of $\dot{\rho}$

$$\dot{Z} = Z_0 \frac{1 + \dot{\rho}}{1 - \dot{\rho}} \tag{160}$$

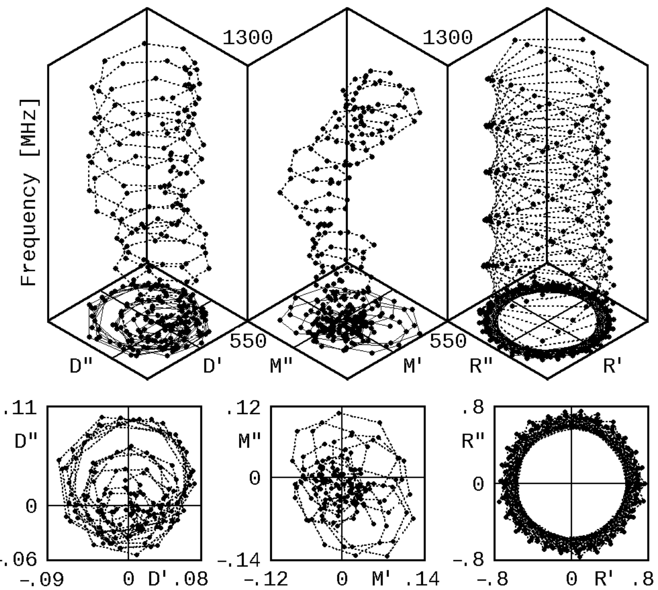

Fig. 10: D, M, R as function of frequency

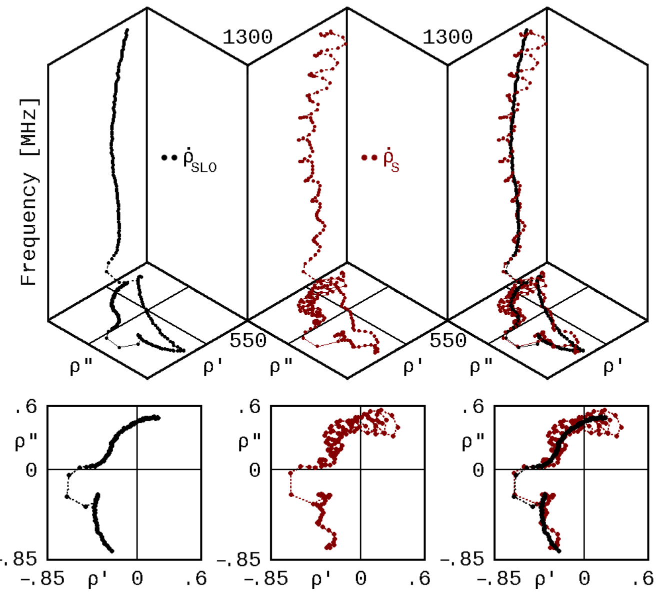

Fig. 13: Antenna's reflection coefficient

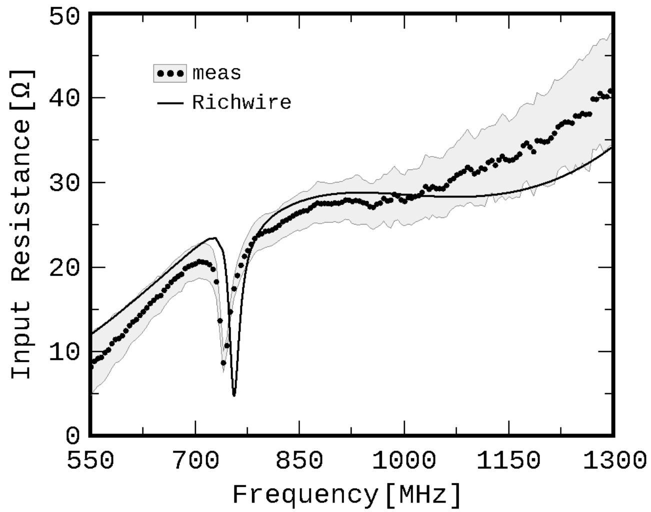

Input impedance real part

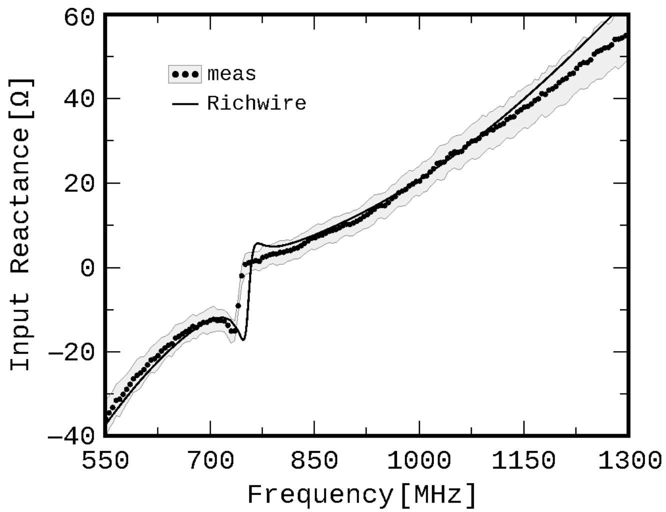

Input impedance imaginary part

Fig. 14: Antenna’s input impedance

or by substitution of $\dot{\rho}$ from ρ-mini (158)

$$\boxed{\dot{Z} = -Z_0 \frac{(\dot{m} - \dot{s})(\dot{l} - \dot{o})}{(\dot{m} - \dot{o})(\dot{s} - \dot{l})}} \quad (161)$$

and as bilinear form

$$\dot{Z} = -Z_0 \frac{\dot{m}(\dot{l} - \dot{o}) + (-\dot{s}(\dot{l} - \dot{o}))}{\dot{m}(\dot{s} - \dot{l}) + (-\dot{o}(\dot{s} - \dot{l}))} \quad (162)$$

Conclusions

This work presented a conceptual model for the reflection measurements of a VNA System. The sets of values of all involved quantities and their corresponding functions, that define the relations between them, are produced in detail.

The transition, from the four-port microwave junction, that represents the measuring operation of a VNA System for reflection measurements, to the reflection full one-port error model, was completely revealed.

The frequency dependent systematic error parameters were expressed, computed, and drawn.

A constructed antenna with a rather complex geometry having cylindrical symmetry was measured and the results for its reflection coefficient $\dot{\rho}$, as well as its directly dependent on $\dot{Z}$ input impedance, were presented.

Finally, although the Lab VNA System includes an externally "Inserted Equipment" IE (that obviously serves the clever ensemble of VNA Systems having a variety of characteristic impedance and connectors, e.g. as it is shown in the simplified T/R Set circuit of Fig. 7, where only the bridge B and its branches need to be changed to 75Ω, while the whole of the other System remains exactly the same 50Ω [37]), its reflection full one-port error model is identical to that of a NanoVNA, where although the IE appears to be a missing component, but in fact it is an internally included device - the full details will be included in a forthcoming paper.

References – Updates – MD5 check

https://www.ftpj.otoiser.org/refs/392.htm

[1] HP, "Vector Measurements of High Frequency Networks", HP publication number 5958-0387, 1989, pp. 3-2 - 3-9

https://ftpj.otoiser.org/refs/392.htm#r1 archive.org/details/vector-measurements-of-high-frequency-networks-paul-schmitz-april-1989-hp-5958-0387

[2] Bianco B., Corana A., Ridella S., Simicich C., "Evaluation of Errors in Calibration Procedures for Measurements of Reflection Coefficient", IEEE Transactions of Instrumentation and Measurement", Vol. IM-27, No. 4, 1978 pp. 354 - 359

[3] Fitzpatrick J., "Error Models for Systems Measurement", Microwave Journal, May 1978, pp. 63 - 66

[4] Young P. R., "Propagation of uncertainty in one-port ANA measurements", ANAMET Report 017, August 1998

[5] Eul H.-J., Schiek B., "A Generalised Theory and New Calibration Procedures for Network Analyser Self-Calibration", IEEE Transactions on Microwave Theory and Techniques, Vol. 39, No. 4, 1991, pp. 724 - 731

[6] Soares R. A., Gouzien P., Legaud P., Follot G., "A Unified Mathematical Approach to Two-Port Calibration Techniques and Some Applications", Transactions on Microwave Theory and Techniques, Vol. 37, No. 11, 1989, pp. 1669 - 1673

[7] "Reference Data for Radio Engineers", Howard W. Sams & Co - ITT, "Ch. 24: Scattering Matrices", 5th Ed., 1972, pp. 1 - 9

[8] Spiegel M. R., "Complex Variables with an introduction to Conformal Mapping and its applications", McGraw-Hill, 1974, pp. 34, 203

[9] Chipman R. A., "Transmission Lines", McGraw Hill, 1968, Ch. 7, pp. 126 - 155

[10] Yannopoulou N. I., Zimourtopoulos P. E., "Measurement Uncertainty in Network Analyzers: Differential Error Analysis of Error Models Part 1: Full One-Port Calibration", FunkTechnikPlus # Journal, Issue 1, Year 1, 2013, pp. 17 - 22

https://ftpj.otoiser.org/refs/392.htm#r10

ftpj.otoiser.org/issues/html/ftpj-issue-01-e4-lo4104-pdfc171-ia1.htm#r12 (1-2)

[11] Yannopoulou N., Zimourtopoulos P., "Total Differential Errors in One-Port Network Analyzer Measurements with Application to Antenna Impedance", Radioengineering, Vol. 16, No. 2, June 2007, pp. 1 - 8

https://ftpj.otoiser.org/refs/392.htm#r11

radioeng.cz/fulltexts/2008/08_01_01_08.pdf

[12] Yannopoulou N. I., Zimourtopoulos P. E., "Comparing a NanoVNA with a LabVNA Part 1: One-Port Measurements", FunkTechnikPlus # Journal, Issue 34, Year 11, 2024, pp. 7 - 41

https://ftpj.otoiser.org/refs/392.htm#r12

ftpj.otoiser.org/issues/html/ftpj-issue-34-lo7532-export-ia1.htm#r341 (34-1)

[13] HP, "8660C Synthesized Signal Generator", HP Operating and Service Manual, May 1979

[14] HP, "86603 RF Section 1-2600MHz", HP Operating and Service Manual, October 1978

[15] HP, "5340 Frequency Counter", HP Operating and Service Manual, September 1975

[16] HP, "8505A Network Analyzer: Operating and Programming", HP Operating and Service Manual, Vol. 1 - A3, Santa Rosa California, USA, August 1979

[17] HP, "8505A Network Analyzer Option 005 Phase Lock", HP Option Supplement Vol. 3 - Chapter E, August 1979

[18] HP, "Using the HP-IB Interface with MS Windows", 1991

[19] HP, "Calculator Control of the 8660A/B/C Synthesized signal generator", HP Application Note 164-2, Aug. 1979

[20] "MS Visual Basic Programming System for Windows v.3.0 (in three books)", Microsoft, 1993

[21] Wolfram Stephen, "The Mathematica Book", Wolfram Research, 1996

[22] Wagner D. B., "Power Programming with Mathematica: The Kernel", McGraw-Hill, 1996

[23] HP, "HP 8505A RF Network Analyzer Basic Measurements", Application Note 219, Palo Alto California, November 1978

https://ftpj.otoiser.org/refs/392.htm#r23

www.hpmemoryproject.org/an/pdf/an_219.pdf

[24] HP, "High Performance RF Network Analyzer", "8505A Specifications", Technical Data, 5952-9268, Palo Alto California, January 1979, pp. 14 - 15

https://ftpj.otoiser.org/refs/392.htm#r24

archive.org/details/high-performance-rf-network-analyzer-hp-8505-a

[25] HP, "8505A Network Analyzer HP Operating and Service Manual", Vol. 1, A1-5 - A1-7, A3-28, A4, August 1979

[26] HP, "8502A Transmission/Reflection Test Set", HP Operating and Service Manual, October 1979

https://ftpj.otoiser.org/refs/392.htm#r26

keysight.com/dk/en/assets/9018-02748/user-manuals/9018-02748.pdf

[27] Kuhn N., "Simplified signal flow graph analysis", Microwave Journal, November 1963, pp. 59 - 66

[28] Collin R. E., "Foundations for Microwave Engineering", John Wiley & Sons Inc., 2nd Ed., 2001, pp. 260 - 268

[29] Keysight, "OPEN/SHORT Response Calibration (reflection test)"

https://ftpj.otoiser.org/refs/392.htm#r29

helpfiles.keysight.com/csg/e5071c/measurement/calibration/basic_calibrations/open_short_response_calibration_reflection_test.htm

[30] Keysight, "Calibration Types and Characteristics"

https://ftpj.otoiser.org/refs/392.htm#r30

helpfiles.keysight.com/csg/e5071c/measurement/calibration/calibration_types_and_characteristics.htm

[31] Keysight Technologies Inc., "909A Coaxial Termination DC to 18 GHz"

https://ftpj.otoiser.org/refs/392.htm#r31

keysight.com/dk/en/assets/7018-03039/technical-overviews/5990-8462.pdf

[32] Maury Microwave, "Precision Microwave Instruments and Components", 1996, p. 132

[33] Yannopoulou N. I., Zimourtopoulos P. E., "Various Loads as Calibration Standards for Vector Network Analyzer Measurements" FunkTechnikPlus # Journal, Issue 38, Year 13, 2025, pp. 13 - 42

https://ftpj.otoiser.org/refs/392.htm#r33

ftpj.otoiser.org/issues/html/ftpjissue38lo7532expor-tia1.htm#r382 (38-2)

[34] Yannopoulou N., Zimourtopoulos P., "ANALYZE: Automated Antenna Measurements, ver. 13", Antennas Research Group, 1993 - 2008

[35] Yannopoulou N. I., "Study of monopole antennas over a multi-frequency decoupling cylinder", PhD Thesis, EECE, DUTh, February 2008 (in Hellenic), pp. 3-27, 5-175 - 5-177

https://ftpj.otoiser.org/refs/392.htm#r35

www.didaktorika.gr/eadd/handle/10442/20920?locale=en

[36] Richmond J. H., "Computer program for thin-wire structures in a homogeneous conducting medium", Publication Year: 1974, NTRS-Report/Patent Number: NASA-CR-2399, ESL-2902-12, DocumentID: 19740020595

https://ftpj.otoiser.org/refs/392.htm#r36

ntrs.nasa.gov/search.jsp?R=19740020595

[37] HP, "8502B 75-Ω Transmission/Reflection Test Set", HP Operating and Service Manual, March 1977

https://ftpj.otoiser.org/refs/392.htm#r37

keysight.com/dk/en/assets/9018-03263/user-manuals/9018-03263.pdf

[This Page Intentionally Left Blank]

ARG NfP AoI
Antennas Research Group
Not-for-Profit Association of Individuals [*]
www.arg.op4.eu – arg@op4.eu
Scheiblingkirchen, Austria

* The Constitution of Greece, Article 12(3) – 2008:
  www.hellenicparliament.gr/en/Vouli-ton-Ellinon/To-Politevma
* The Hellenic Supreme Court of Civil and Penal Law:
  www.areiospagos.gr/en – Court Rulings:Civil|A1|511|2008

FRONT COVER VIGNETTE

A faded synthesis of an anthemion rooted in a meandros

The thirteen-leaf is a symbol for a life tree leaf.
"Herakles and Kerberos", ca. 530–500 BC,
by Paseas, the Kerberos Painter,
Museum of Fine Arts, Boston.

www.mfa.org/collections/object/plate-153852

The simple meandros is a symbol for eternal immortality.
"Warrior with a phiale", ca. 480–460 BC,
by Berliner Maler,
Museo Archeologico Regionale "Antonio Salinas" di Palermo.

commons.wikimedia.org/wiki/File:Warrior_MAR_Palermo_NI2134.jpg